

model the $\frac{1}{2}^+$ state in ^{17}O at 6.38 MeV and the $\frac{3}{2}^+$ state at 7.30 MeV are interpreted in terms of three-particle two-hole and five-particle four-hole excitations. Although this approach gives reasonable agreement with experiment, there are difficulties. For example, even though they carry the expansion to obtain core excitations in even numbers of particle and hole states through four-particle four-hole states, they find more terms must be included to obtain correct transition rates between states or to obtain the correct quadrupole moment of ^{17}O in its ground state. The approach¹ based on the cluster model has no trouble in giving these transition rates and the quadrupole moment correctly; moreover, it gives an adequate description of the position and widths of the states of ^{17}O below 5.2 MeV. The theoretical problem associated with the cluster model is that of finding its connection with the shell model which, because of its successful correlation of so many properties of nuclei, is generally believed to be the basic starting point for any description of nuclei. That there

is such a connection between the cluster model and the shell model has been recognized for a long time.³⁴ In a recent review paper, this connection is explored in some detail.³⁵

ACKNOWLEDGMENTS

We wish to acknowledge the assistance we had from Dr. J. A. Biggerstaff and R. P. Cumby who helped us in checking out the pulse-shape discriminator circuits, and that from Mrs. Eugene Patterson who altered the phase-shift computer program to fit the special cases arising in ^{16}O neutron scattering. We wish also to thank S. T. Thornton, R. L. Kernell, W. T. Newton, R. A. Robinson, and W. C. H. White who at various times helped us in taking data during the course of this experiment.

³⁴ J. K. Perring and T. H. R. Skyrme, Proc. Phys. Soc. (London) **69A**, 600 (1956).

³⁵ V. G. Neudachin and Yu. F. Smirnov, At. Ener. Rev. **3**, 157 (1965).

Fluctuations in Excitation Functions for $^{12}\text{C}(^{16}\text{O}, \alpha)^{24}\text{Mg}^\dagger$

M. L. HALBERT, F. E. DURHAM,* AND A. VAN DER WOUDE†

Oak Ridge National Laboratory, Oak Ridge, Tennessee

(Received 29 March 1967)

Cross sections were measured at five angles for alpha-particle groups from the reaction $^{12}\text{C}(^{16}\text{O}, \alpha)^{24}\text{Mg}$. The measurements were made with 40–50-keV resolution over energy intervals as long as 9.9 MeV (c.m.). The data provided large samples for fluctuation analyses over compound-nucleus excitation energies from about 25 to 35 MeV. The average coherence width, which is dominated by compound states with $J \sim 10$, was found to be about 118 keV. It does not vary significantly with exit channel, angle, or excitation energy in the compound nucleus. Most of the data are well represented by the simple Ericson–Brink–Stephen statistical model and show no significant direct-interaction component. A pronounced peak appearing in several of the excitation functions near 31.8-MeV bombarding energy is not consistent with this model.

I. INTRODUCTION

FOR a simplified stochastic model of the compound nucleus at high excitation energies, Ericson^{1,2} and Brink and Stephen³ have shown that interference among overlapping compound levels will cause cross sections to fluctuate rapidly as a function of energy. Statistical analysis of the deviations from average behavior enables one to determine certain average properties of the compound system that are difficult or impossible to obtain otherwise, for example, the width Γ of the compound states.

† Research sponsored by the U. S. Atomic Energy Commission under contract with the Union Carbide Corporation.

* Temporary employee from Tulane University; partial support received from Oak Ridge Associated Universities.

‡ On leave 1963–1965 from the University of Groningen, The Netherlands.

¹ T. Ericson, Phys. Rev. Letters **5**, 430 (1960).

² T. Ericson, Ann. Phys. (N. Y.) **23**, 390 (1963).

³ D. M. Brink and R. O. Stephen, Phys. Letters **5**, 77 (1963).

The present report describes measurements and statistical analyses of excitation functions for $^{12}\text{C}(^{16}\text{O}, \alpha)^{24}\text{Mg}$ for alpha-particle groups going to the low-lying levels of ^{24}Mg . The excitation energies of the ^{28}Si compound nucleus were in the range from 25.6 to 35.5 MeV. Data were taken at intervals of 43 keV (center-of-mass) with an energy resolution of 40–50 keV (c.m.). The excitation functions were obtained at five laboratory angles, nominally 0° , 20° , 69° , 149° , and 178° . Much more complete angular distributions were measured earlier at a number of energies; these are described in the following paper.⁴ Reference 4 also contains data taken with 15-keV resolution to check for narrower structure (none was found).

A summary of the excitation-function measurements is given in Table I. The alpha-particle groups studied

⁴ M. L. Halbert, F. E. Durham, C. D. Moak, and A. Zucker, following paper, Phys. Rev. **162**, 919 (1967).

TABLE I. Summary of experimental measurements. All energies are in MeV.

Nominal lab angle	Bombarding energy span	Center-of-mass energy span	²⁸ Si excitation energy span	Groups studied	Mean center-of-mass angles	
					Lowest ¹⁶ O energy	Highest ¹⁶ O energy
0°	20.6-43.7	8.84-18.75	25.6-35.5	α ₀	1.5°	1.5°
	20.6-43.7	8.84-18.75	25.6-35.5	α ₁	1.5°	1.5°
	20.6-43.7	8.84-18.75	25.6-35.5	α ₂ +α ₃	1.5°	1.5°
	20.6-43.7	8.84-18.75	25.6-35.5	α ₅	1.6°	1.6°
	20.6-43.7	8.84-18.75	25.6-35.5	α ₆	1.6°	1.6°
20°	20.6-43.7	8.84-18.75	25.6-35.5	α ₀	27.0°	27.9°
	20.6-43.7	8.84-18.75	25.6-35.5	α ₁	27.3°	28.2°
	20.6-43.7	8.84-18.75	25.6-35.5	α ₂ +α ₃	28.2°	28.7°
	20.6-43.7	8.84-18.75	25.6-35.5	α ₄	28.6°	28.9°
	22.6-43.7	9.70-18.75	26.5-35.5	α ₅ +α ₆	29.0°	29.1°
69°	21.0-37.9	9.00-16.24	25.8-33.0	α ₀	88.4°	90.7°
	21.0-37.9	9.00-16.24	25.8-33.0	α ₁	89.4°	91.4°
	21.0-37.9	9.00-16.24	25.8-33.0	α ₂ +α ₃	91.8°	93.1°
	21.0-37.9	9.00-16.24	25.8-33.0	α ₄	92.9°	93.9°
	21.0-37.9	9.00-16.24	25.8-33.0	α ₅ +α ₆	94.1°	94.5°
149°	21.0-27.5	9.00-11.79	25.8-28.5	α ₀	159.6°	160.1°
	21.0-27.5	9.00-11.79	25.8-28.5	α ₁	160.1°	160.6°
	21.0-27.5	9.00-11.79	25.8-28.5	α ₂ +α ₃	161.3°	161.7°
	33.0-37.9	14.14-16.24	30.9-33.0	α ₀	160.5°	160.8°
	33.0-37.9	14.14-16.24	30.9-33.0	α ₁	160.9°	161.1°
178°	21.0-27.5	9.00-11.79	25.8-28.5	α ₂ +α ₃	161.9°	162.0°
	21.0-27.5	9.00-11.79	25.8-28.5	α ₀	179.0°	179.1°
	21.0-27.5	9.00-11.79	25.8-28.5	α ₁	179.1°	179.1°
	21.0-27.5	9.00-11.79	25.8-28.5	α ₂ +α ₃	179.1°	179.1°
	33.0-37.9	14.14-16.24	30.9-33.0	α ₀	179.1°	179.1°
33.0-37.9	14.14-16.24	30.9-33.0	α ₁	179.1°	179.1°	

correspond to the following well-known levels of ²⁴Mg:

α ₀	ground state	0 ⁺
α ₁	1.37-MeV level	2 ⁺
α ₂	4.12-MeV level	4 ⁺
α ₃	4.23-MeV level	2 ⁺
α ₄	5.22-MeV level	3 ⁺
α ₅	6.00-MeV level	4 ⁺
α ₆	6.44-MeV level	0 ⁺

The α₂ and α₃ groups were unresolved. The α₅ and α₆ could be resolved at 0°, but not at other angles because of the kinematic variation of particle energy across the aperture of the counter.

The longest energy spans, about 84 Γ, are for the 0° and 20° data. The 69° data cover about 61 Γ. The availability of data over such long intervals minimizes corrections for finite-sample effects⁵⁻⁷ and thereby increases the reliability of the parameters extracted by the statistical analysis. Other excitation function data for much smaller samples were presented earlier.⁸ The strong influence of the finite-sample effects was not then realized, and the conclusion reached at that time about the percentage of direct interaction is not valid. The present results show that the reaction proceeds predominantly via a compound nucleus.

⁵ M. Böhning, in *Comptes Rendus du Congrès International de Physique Nucléaire*, edited by P. Gugenberger (Centre National de Recherche Scientifique, Paris, 1964), Vol. II, p. 697; T. Mayer-Kuckuk, Hercegovi Lectures, 1964 (unpublished).

⁶ I. Hall, *Phys. Letters* **10**, 199 (1964).

⁷ W. R. Gibbs, *Phys. Rev.* **139**, B1185 (1965).

⁸ M. L. Halbert, F. E. Durham, C. D. Moak, and A. Zucker, *Nucl. Phys.* **47**, 353 (1963).

II. EXPERIMENTAL METHOD

The Oak Ridge tandem accelerator produced the ¹⁶O beams; the 4⁺ beam was used up to about 33 MeV, the 5⁺ beam to 41 MeV, and the 6⁺ beam at higher energies. The targets were self-supporting evaporated films of natural carbon.

Alpha particles from the target were detected in silicon surface-barrier counters. Two detectors were used simultaneously to take data at 0° and 20° for bombarding energies from 20.6 to 43.7 MeV, over the course of two runs several months apart. Later, a single counter at 69° was used for the 27.6-32.9-MeV span. Finally, counters at 69°, 149°, and 178° were used simultaneously for measurements from 21.0 to 27.5 MeV and 33.0 to 37.9 MeV. The sensitive depth of each detector was adjusted so that proton and deuteron pulses did not appear in the region of interest. A portion of a zero-degree spectrum is shown in Fig. 1. At 20°, the counter bias was inadvertently left too high as the beam energy was being reduced, and the α₅+α₆ peak fell within the proton-deuteron region of the spectrum. Thus the 20° data could not be used below 22.6-MeV bombarding energy.

Thin nickel foils were placed in front of the detectors to stop scattered ¹⁶O and other heavy ions. These were 4 to 10 mg/cm² thick, the thicker ones being used at forward angles. At back angles the alpha-particle energies were only a few MeV, and their range was comparable with that of ¹⁶O ions back-scattered from the beam stopper (see below). For this reason it was not

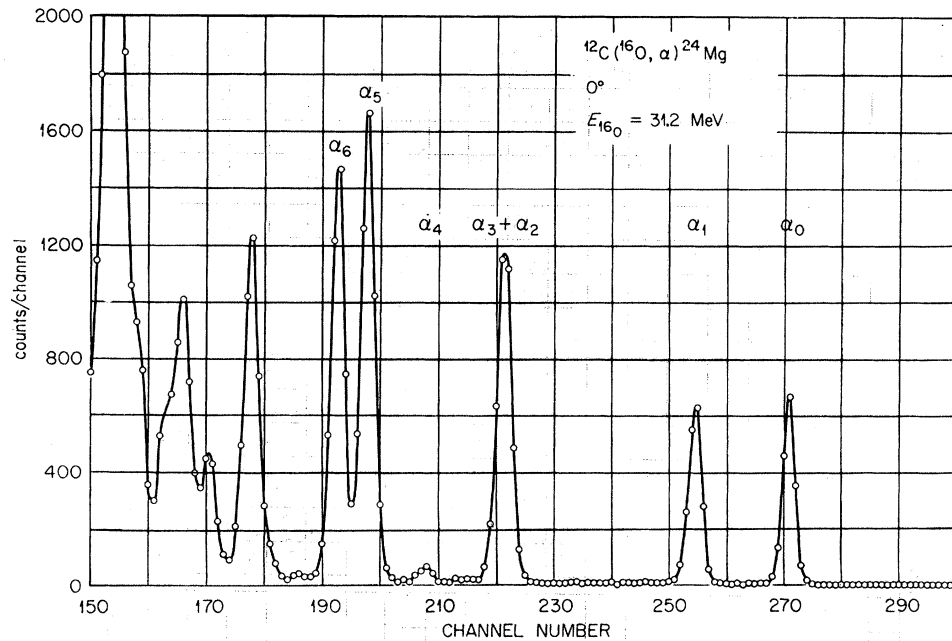


FIG. 1. Typical spectrum at 0° .

possible to obtain data at 178° on the $\alpha_2 + \alpha_3$ group at the higher bombarding energies.

For the 0° and 20° data, the beam direction was determined to 0.1° by taking advantage of the strong angular dependence of the cross sections.⁴ The counting rate was measured for several alpha groups at angles near the expected 0° position; the true zero angle corresponded to an extremum in the counting rates versus angle. The angles for the 69° and 149° detectors were measured with a protractor to an accuracy of about $\pm 1^\circ$. The detector placed at the nominal 178° angle was an annulus with a central hole of 4-mm diam through which the beam entered the target chamber. The sensitive area of this detector was actually centered at an angle of 178.5° , with a half-angle of 0.5° . The detector centered at 0° subtended a cone of half-angle 1.6° , corresponding to an average angle of 1.1° for the nominal 0° excitation function. The detectors at 20° , 69° , and 149° had circular apertures which subtended half-angles of approximately 2° . The effective center-of-mass angles for all the detectors are given in Table I for the various excited states and bombarding energies.

The target thickness was crucial in determining the entrance-channel energy resolution. The initial thickness of each target was determined by means of an optical densitometer.⁸ Typical values were $8\text{--}12 \mu\text{g}/\text{cm}^2$. When new targets were installed, intercomparisons of counting rates at a standard energy were made to establish the relative thicknesses; the results were in agreement with the optical-density measurements. For the 0° and 20° data, the target was perpendicular to the beam. The other data were taken with the normal to the target plane making an angle of 12° or 13° with the beam direction.

Buildup of carbon on the portion of the target struck by the beam was a serious problem. Typically, after $2\frac{1}{2}$ hours of bombardment by 200 nA of $^{16}\text{O}^{4+}$, the increase in counting rate at a given energy was about 30%. To maintain adequate energy resolution, it was necessary to expose a fresh target area at frequent intervals. The buildup was checked every 2 to 4 h, after each series of about ten successive energies had been run, by returning to a standard beam energy and comparing the alpha-particle yields before and after each series. In calculating the cross sections, it was assumed that the rate of buildup was constant within each series.

The effective target thicknesses thus ranged from 8 to $16 \mu\text{g}/\text{cm}^2$. The stopping power curves given by Northcliffe⁹ for ^{16}O in carbon indicate an energy loss ranging from $9.0 \text{ keV}/\mu\text{g}\text{-cm}^2$ at 20 MeV to $6.7 \text{ keV}/\mu\text{g}\text{-cm}^2$ at 40 MeV. The spread in bombarding energy due to target thickness thus varied from 54 keV (23 keV c.m.) near 40 MeV for the thinnest targets to 154 keV (66-keV c.m.) for a few runs at low energies. The average energy resolution was about 45 keV (c.m.).

Nonuniformity of the target would influence the effective energy resolution. Exploration with the optical densitometer with a spatial resolution comparable to the area of the beam spot showed that the targets were uniform within 10 or 20%. Examination of foils under a microscope with several magnifications up to $250\times$ revealed no irregularities.

In some of the spectra a very small peak (5–10 counts) was seen above the α_0 group. This peak may be due to ground-state alphas from reactions with ^{16}O impurity in the target. It is important to ascertain whether the impurity might cause an error in the esti-

⁹ L. C. Northcliffe, *Ann. Rev. Nucl. Sci.* 13, 69 (1963).

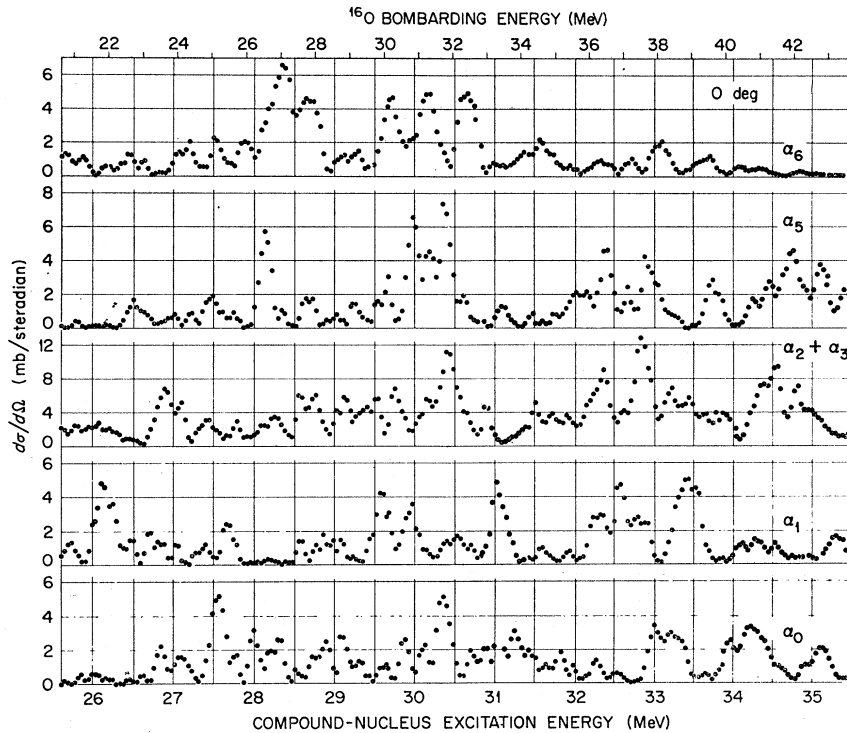


FIG. 2. Excitation functions for $^{12}\text{C}(^{16}\text{O}, \alpha)^{24}\text{Mg}$ at 0° .

mate of target thickness. Elastic scattering from fresh targets showed no scattering peak from oxygen impurity. The buildup of oxygen during a series of runs is difficult to estimate accurately because of the very low counting rates, but it does not appear to be larger than that for the carbon. Consequently, the energy loss in the target estimated above for the carbon alone should be sufficiently accurate.

To stop the beam, nickel foils totaling 10 to 20 mg/cm^2 were attached to the target frame immediately behind the carbon foil. The entire assembly was insulated from ground and connected to the current integrator. Therefore, the change in average charge of the ^{16}O ions as they passed through the carbon was of no concern. Secondary electrons were collected by maintaining the target assembly and beam stopper at a potential of +300 V. In addition, permanent magnets were placed on the top of the scattering chamber to aid in electron collection. The accuracy of beam-current integration was better than 5%.

The absolute cross sections are believed to be accurate to about $\pm 25\%$. The dominant contribution to this estimated error is the uncertainty in target thickness. Random errors due to counting statistics for the data at 0° , 20° , 69° , 149° , and 178° may be estimated from the relation that 1 mb/sr corresponds to approximately 400, 400, 1000, 500, and 250 counts, respectively.

The data were obtained in several runs over a period of more than a year. The analyzing magnet governing the beam energy was not precisely calibrated and deviations of about 100 keV in the nominal beam energy

were noted from run to run. These shifts were detected by comparing plots of excitation functions which partially overlapped previously obtained data at the same angle. Because of the strong fluctuations in all the cross sections at 0° , the various portions of the data could easily be tied together to within 10 keV. It was decided to standardize on the energy scale of the angular-distribution data⁴ near 31 MeV because those data were actually obtained first. The angular distributions included measurements at 20° but not at 0° . Therefore, the 20° data obtained simultaneously with the 0° data were used to shift the entire 0° and 20° excitation functions to agree with the energy scale of Ref. 4; the required shift was +30 keV.

For the data obtained later at 69° , 149° , and 178° , adjustment to the energy scale of Ref. 4 is more difficult. The angle is known best for the 178° data, but the angular distributions do not extend to such large angles. Slight differences in the choice of laboratory angle between the data of Ref. 4 and the present results, plus the uncertainty of about 1° , make it impossible to match the two scales exactly. However, it seems that the two scales are consistent within 100 keV.

III. RESULTS

The alpha-particle excitation functions at the five angles are given in Figs. 2–6. The points shown are center-of-mass cross sections. The data were obtained at fixed laboratory angle; the corresponding center-of-mass angle depends on energy, as shown in Table I. The largest effect is at 69° (lab) for α_0 .

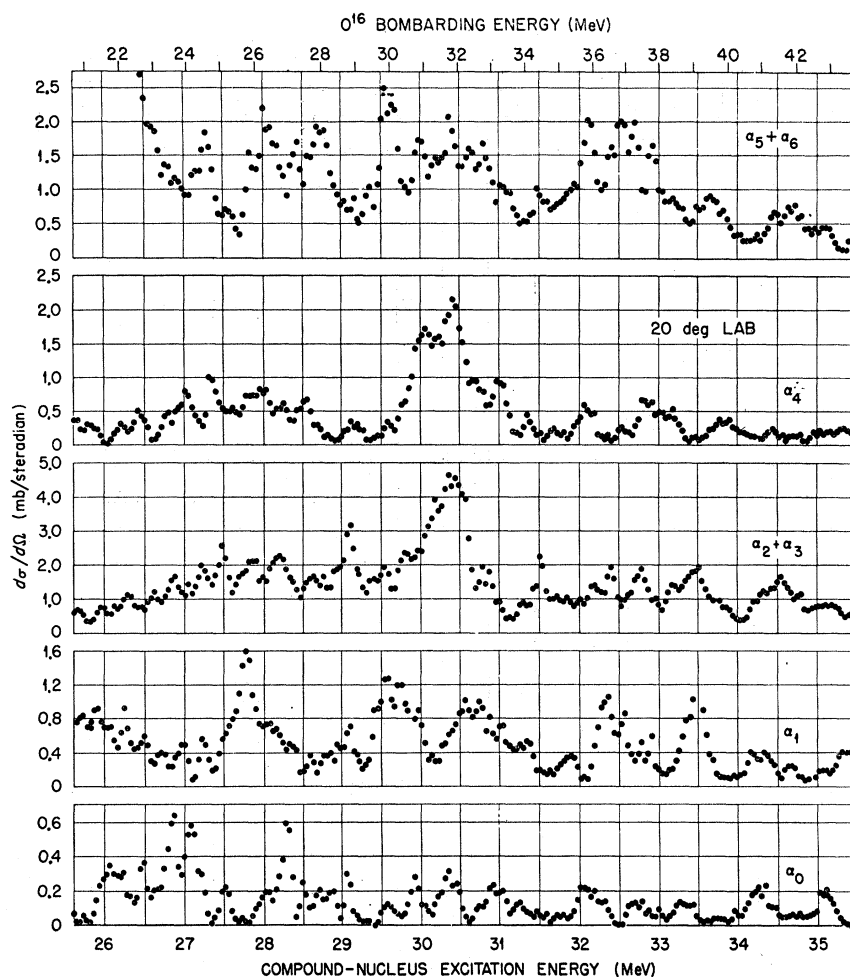


FIG. 3. Excitation functions for $^{12}\text{C}(^{16}\text{O}, \alpha)^{24}\text{Mg}$ at 20° (lab).

IV. ANALYSIS AND DISCUSSION

A. Basis of Fluctuation Analysis

The fluctuations contain useful information about certain average properties of the participating compound states. The coherence width of the fluctuations has been shown to be equal to the average decay width Γ of the compound states.² The nonfluctuating fraction y of the cross section (identified as the direct-interaction component) can be determined by a statistical analysis. To extract these quantities from the data, we compare the experimental results with theoretical predictions based on the following simplified model of the compound states, due to Ericson² and Brink and Stephen.³

The reaction amplitude is assumed to be a sum of uncorrelated, strongly overlapping Breit-Wigner resonances of average width Γ , plus a nonfluctuating term. The real and imaginary parts of the resonance amplitudes are assumed independent and normally distributed with mean values of zero. The system is assumed to be stationary—that is, the expectation value of an energy average is independent of where the range of averaging begins.

This model is a member of the class of “ S -matrix models” discussed recently by Moldauer.¹⁰ That is, the assumptions about the resonance amplitudes needed for evaluation of the statistical properties of the S matrix are chosen in part for computational convenience and may not be completely realistic. The “ R -matrix models,”¹⁰ on the other hand, are those in which well-established statistical properties of the compound states are used to generate the pole expansion of the S matrix by means of the R -matrix theory. Certain results differ markedly from those of the simplified model if strongly absorbed channels are involved.¹⁰ Under these circumstances the excitation functions will occasionally show peaks considerably stronger and broader than the average. These peaks tend to occur at the same energy in several exit channels, and they are associated with a definite angular momentum. Calculations with the R -matrix models are very complicated and at present quantitative predictions have not been developed to the same extent as for the Ericson-Brink-Stephen model.

¹⁰ P. A. Moldauer, Phys. Rev. Letters 18, 249 (1967).

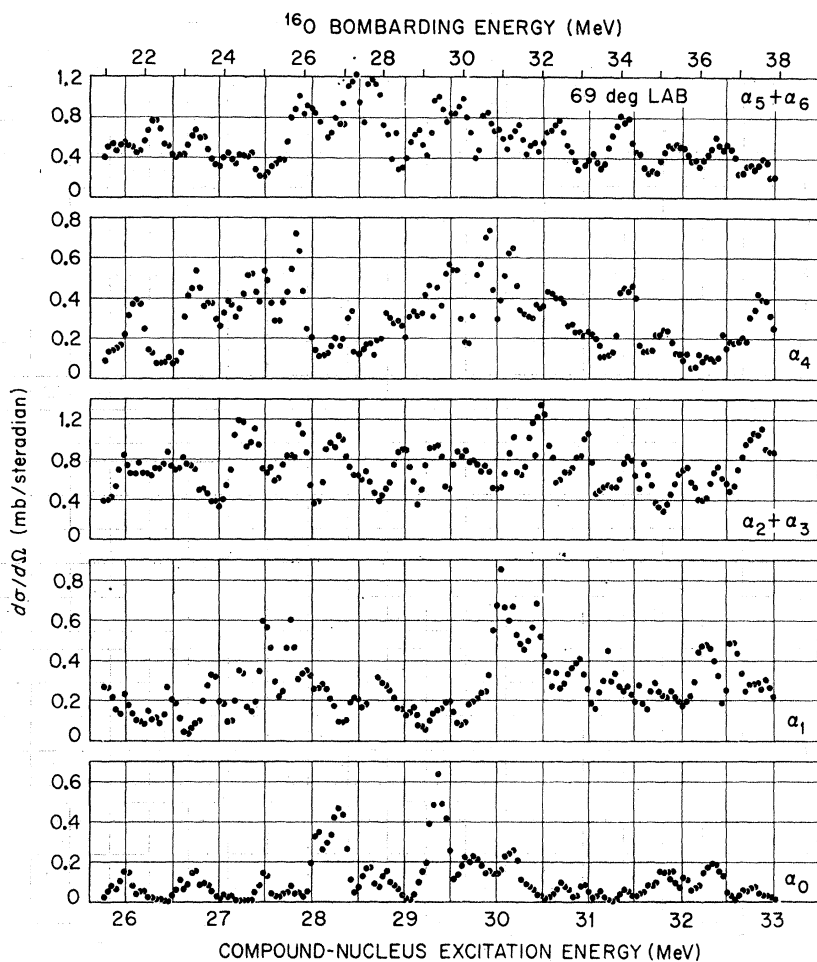


FIG. 4. Excitation functions for $^{12}\text{C}(^{16}\text{O}, \alpha)^{24}\text{Mg}$ at 69° (lab).

Therefore only brief references to the more accurate class of models appear in the following discussion.

The strong-overlap condition is stated by $\Gamma \gg D$, where D is the average spacing of the compound-system resonances. The question arises as to the value of Γ/D in the ^{28}Si compound system studied here and the effects of incomplete overlap on the quantities de-

rived from the fluctuation analysis. These matters are treated in Appendix A; it is concluded there that Γ/D is sufficiently large for these effects to be unimportant.

For nonzero spins in the entrance or exit channels, one considers in this simple model N such amplitudes of equal intensity, each statistically independent of the

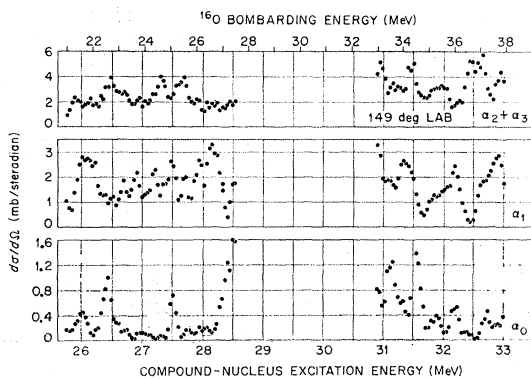


FIG. 5. Excitation functions for $^{12}\text{C}(^{16}\text{O}, \alpha)^{24}\text{Mg}$ at 149° (lab).

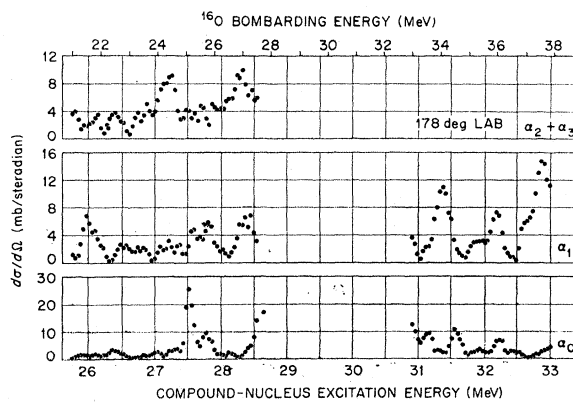


FIG. 6. Excitation functions for $^{12}\text{C}(^{16}\text{O}, \alpha)^{24}\text{Mg}$ at 178° (lab).

TABLE II. Results for full energy ranges for each alpha-particle group. N is the estimated number of effective channels. Γ_A includes corrections for finite-sample and energy-resolution effects. M is the number of maxima in each excitation function.

Angle (lab)	Group	N	Bombarding energy span (MeV)	Average cross section (mb/sr)	Autocorrelation widths		M	Γ_M (keV)
					Observed Γ_{obs} (keV)	Corrected Γ_A (keV)		
0°	α_0	1	20.6–43.7	1.37	105	108	41±2	109
	α_1	1	20.6–43.7	1.33	125	129	42±1	106
	$\alpha_2+\alpha_3$	2	20.6–43.7	3.69	129	131	38±3	118
	α_5	1	20.6–43.7	1.47	133	137	40±4	112
	α_6	1	20.6–43.7	1.36	201	207	37±6	121
	20°	α_0	1	20.6–43.7	0.14	108	111	38±4
α_1		3	20.6–43.7	0.52	180	182	40±4	110
$\alpha_2+\alpha_3$		8	20.6–43.7	1.44	300	301	42±3	103
α_4		3	20.6–43.7	0.44	410	414	41±4	108
$\alpha_5+\alpha_6$		6	22.6–43.7	1.09	204	206	39±4	102
69°		α_0	1	21.0–37.9	0.11	110	116	30±3
	α_1	3	21.0–37.9	0.27	126	129	30±3	107
	$\alpha_2+\alpha_3$	8	21.0–37.9	0.71	86	87	29±4	109
	α_4	3	21.0–37.9	0.30	111	114	32±4	101
	$\alpha_5+\alpha_6$	6	21.0–37.9	0.57	139	142	34±5	94
	149°	α_0	1	21.0–27.5	0.32	123	146	11±1
α_0		1	33.0–37.9	0.46	114	143	8±1	115
α_1		3	21.0–27.5	1.76	74	83	11±2	110
α_1		3	33.0–37.9	1.67	110	128	6±1	151
$\alpha_2+\alpha_3$		8	21.0–27.5	2.30	105	114	15±2	79
$\alpha_2+\alpha_3$		8	33.0–27.9	3.45	86	98	10±2	89
178°	α_0	1	21.0–27.5	3.73	95	113	11±1	112
	α_0	1	33.0–37.9	4.11	95	119	7±1	131
	α_1	1	21.0–27.5	2.73	116	138	14±2	88
	α_1	1	33.0–37.9	4.96	131	164	5±1	183
	$\alpha_2+\alpha_3$	2	21.0–27.5	4.34	174	198	12±2	102

others. The fluctuations are at a maximum for $N=1$ and are damped as N increases. An approximation to N for differential cross sections may be obtained by counting the number of magnetic substates which can contribute ($+m$ and $-m$ are counted only once). This assumes that the “basic cross sections”¹¹ are independent and of equal intensity. Limitations on the accuracy of such an estimate have been discussed recently by Gibbs¹²; in the present case the angular momenta involved, ~ 10 , are high enough⁴ that these limitations do not apply. In $^{12}\text{C}(^{16}\text{O}, \alpha)^{24}\text{Mg}$, all initial and final spins are zero except for some excited levels of the residual nucleus. If the excited level of ^{24}Mg has spin j and parity $(-)^j$, then the above approximation leads to $N=j+1$. For unnatural-parity levels [parity= $(-)^{j+1}$], the $m=0$ component vanishes at all angles,¹¹ and then $N=j$. These N values apply to intermediate angles. At 0° and 180°, all $m \neq 0$ cross sections vanish so that $N=1$. Unnatural-parity levels give no yield at 0° or 180°.^{11,13}

The values of N estimated in this way are given in Table II. For the $\alpha_2+\alpha_3$ and $\alpha_5+\alpha_6$ groups, the N values for the individual levels were added together. This procedure is valid if the cross sections for the individual levels are equal. Some justification for this assumption is furnished by the resolved α_5 and α_6 data at 0°: their average cross sections are, in fact, nearly equal. The $\alpha_2+\alpha_3$ group at 0° is somewhat more than twice as intense as the other groups.

¹¹ J. P. Bondorf and R. B. Leachman, Kgl. Danske Videnskab. Selskab, Mat. Fys. Medd. 34, No. 19 (1965).

¹² W. R. Gibbs, Phys. Rev. 153, 1206 (1967).

¹³ A. E. Litherland, Can. J. Phys. 39, 1245 (1961).

For the “zero-degree” data, the effective angle is actually about 1.5° (c.m.), as shown in Table I. Therefore, m values other than $m=0$ can contribute to the measured yields. A small peak due to the unnatural-parity α_4 group can, in fact, be seen at some energies (see Fig. 1). The effective N values for the other levels of nonzero spin should consequently be somewhat larger than unity. The increase in N for a 2^+ state was estimated for the term in the reaction amplitude corresponding to a total angular momentum of 10. The $m=\pm 1$ contributions are the first to become significant as θ increases since $Y_l^m(\theta, \varphi) \sim (\sin\theta)^m$ for small θ . The sum of the $m=\pm 1$ terms relative to the one for $m=0$ was obtained by multiplying the relevant vector-addition coefficients and spherical harmonics, and then adding the products for all the possible l values. This procedure implies that the elements of the collision matrix are not dependent on the angular-momentum quantum numbers. This assumption is not true, of course, but the magnitude of N near $\theta=0$ is rather insensitive to it. At 1.5° the effective N value was found to be 1.04. This result was checked by the following simple consideration. For $y=0$, the angular cross-correlation function is equal to $1/N_{\text{eff}}$.¹⁴ If we use the surface-emission-model prediction¹⁴ of this function with the observed⁴ coherence angle of 6.2°, the value for N_{eff} at 1.5° is again 1.04. The effect is thus small, and N for the “zero-degree” data will be taken equal to unity in the

¹⁴ D. M. Brink, R. O. Stephen, and N. W. Tanner, Nucl. Phys. 54, 575 (1964).

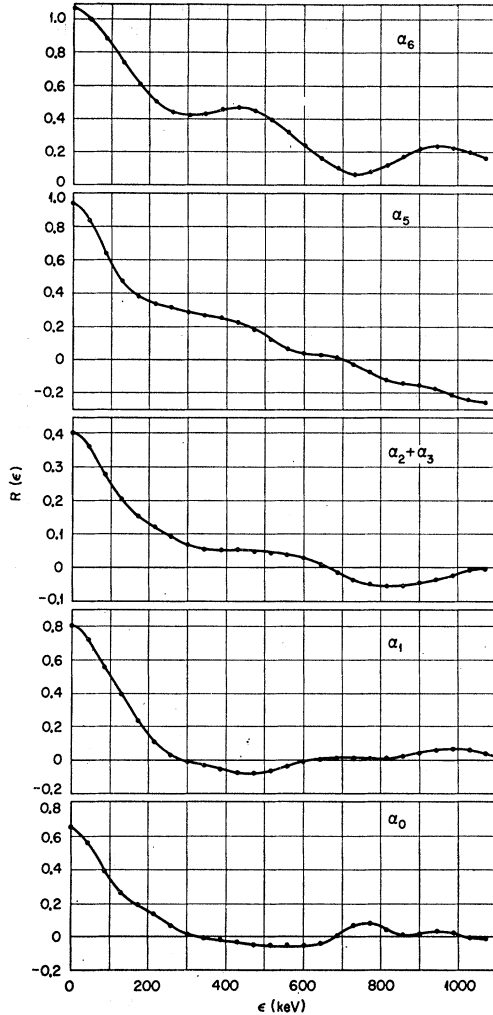


FIG. 7. Autocorrelation functions for the data at 0° .

rest of this paper. The same simplification will be made for the 178° data.

Effects arising from the finite length I of excitation functions are characterized by the sample-size parameter n representing the effective number of statistically independent pieces of data in this energy interval. As outlined in Appendix B, the sample size is given to a very good approximation by

$$n = I/(\pi\Gamma) + 1. \quad (1)$$

All the finite-sample corrections were made with the initial guess that $\Gamma = 115$ keV. The over-all average of the experimental results came out sufficiently close to this to make iteration unnecessary.

It is sometimes useful to combine results at different angles. The question arises of whether the data being combined are statistically independent. The coherence angle, a measure of the angular cross correlation of the fluctuations,¹⁴ provides an answer. It is shown in Ref. 4

that the average coherence angle averaged over all the alpha-particle groups is 6.2° near the midpoint of these excitation functions. The excitation functions at 149° and 178° are the two which come closest in center-of-mass angle. Their 19° (c.m.) separation is three times the coherence angle, and is probably sufficient to guarantee that the results from these two excitation functions are substantially independent. The next closest pair of angles (0° and 20° lab) are more than 4.5 coherence angles apart.

In what follows, the expectation value of the stochastic variable Z will be designated by \bar{Z} or by $\mathcal{E}\{Z\}$. Its variance (square of its standard deviation) is defined by

$$\text{var}Z = \mathcal{E}\{Z^2\} - \bar{Z}^2. \quad (2)$$

The relative standard deviation is

$$\text{RSD}(Z) = (\text{var}Z)^{1/2}/\bar{Z}. \quad (3)$$

An energy average over the interval I will be designated by $\langle Z \rangle_I$.

B. Determination of Γ

The value of Γ was obtained in two ways, from the autocorrelation width² and from the number of maxima per unit energy.³

The autocorrelation function is defined by the expression

$$\mathcal{E}\{\sigma(E)\sigma(E+\epsilon)\}/[\mathcal{E}\{\sigma(E)\}]^2 - 1.$$

The expectation values called for cannot be obtained from finite samples of experimental data, so it is necessary to introduce some estimate of the autocorrelation function. The following expression, similar to one suggested by Böhning,⁵ was used as an estimator of the autocorrelation function:

$$R(\epsilon) = \frac{\langle \sigma(E)\sigma(E+\epsilon) \rangle_{I_1}}{\langle \sigma(E) \rangle_{I_1} \langle \sigma(E) \rangle_{I_2}} - 1. \quad (4)$$

In this paper, σ will always refer to a differential cross section per unit solid angle. The intervals I_1 and I_2 are $(E_1, E_2 - \epsilon)$ and $(E_1 + \epsilon, E_2)$, respectively, where E_1 and E_2 are the lowest and highest energies under consideration.

For the simplified model described above, the expectation value of (4), $\bar{R}(\epsilon)$, approaches a Lorentzian with width at half-maximum of Γ as the energy span, $E_2 - E_1$, increases without limit.^{3,5} For finite excitation functions, $\bar{R}(\epsilon)$ shows an undershoot.⁵ Consequently, the observed autocorrelation width tends to be smaller than the true Γ and a correction must be made. Furthermore, finite sample size leads to a spread of values about $\bar{R}(\epsilon)$. This distribution of values of $R(\epsilon)$ manifests itself in part by oscillations⁵ of $R(\epsilon)$ for large ϵ . It may be mentioned that even these oscillations contain information about the average properties of the system:

TABLE III. Relative standard deviations of Γ_M and Γ_A . The expected values were obtained from Ref. 17 for Γ_M and from (B19) for Γ_A . Values of $\text{RSD}(\Gamma_A)$ in parentheses were obtained by omission of excessively large values.

Angle (lab)	Bombarding energy span (MeV)	RSD(Γ_M)		RSD(Γ_A)	
		Experimental	Expected	Experimental	Expected
0°	20.6–43.7	0.05	0.07	0.24 (0.09) ^a	0.13 (0.13) ^a
20°	20.6–43.7 ^b	0.05	0.07	0.43 (0.24) ^c	0.11 (0.12) ^c
69°	21.0–37.5	0.06	0.08	0.15	0.13
149°	21.0–27.5	0.15	0.14	0.23	0.20
178°	33.0–37.9	0.22	0.17	0.15	0.23
	21.0–27.5	0.10	0.14	0.24	0.23
	33.0–37.9	0.17	0.17	0.16	0.27

^a Omitting α_6 .

^b Interval for $\alpha_5 + \alpha_6$ is 22.6–43.7 MeV.

^c Omitting $\alpha_2 + \alpha_3, \alpha_4,$ and $\alpha_5 + \alpha_6$.

They have been used to extract Γ from experimental data.¹⁵

Examples of portions of the autocorrelation functions for small ϵ are given in Fig. 7; these are for the zero-degree data. The undershoot and oscillations are evident even for these relatively long intervals ($\sim 84^\circ$). The α_6 curve does not cross the axis; this may be due to the nonstationary character of its excitation function.¹⁶ It is evident from Fig. 2 that the α_6 cross section at high energies tends to be smaller than at low energies. The effect of a slow variation of the average cross section has been studied in some detail^{6,16} and it can be eliminated. In this work such effects were encountered occasionally, but no attempt was made to correct the data systematically because the peak-counting method provides more reliable values of Γ with less effort, as will be discussed later.

The experimentally observed autocorrelation widths, Γ_{obs} , are given in Table II. These are the values of ϵ for which $R(\epsilon)/R(0) = \frac{1}{2}$. Before equating these to the compound-state width Γ , two corrections must be made. The experimental energy resolution $\Delta E \approx 45$ keV (c.m.) increases Γ_{obs} by 3.8%, according to the following expression^{17,18}:

$$\Gamma_{\text{obs}} \cong \Gamma \left[1 + \frac{1}{4} \left(\frac{\Delta E}{\Gamma} \right)^2 + \dots \right]. \quad (5)$$

The other correction is for the finite-sample bias referred to above. Appendix B contains a discussion of this effect. The observed autocorrelation widths were corrected by using (B13). For $N=1$, the bias is 30% for the shortest interval and 7% for the longest. The effect is smaller for $N>1$.

The results corrected for these two effects are designated by Γ_A and are listed in Table II. Four values seem excessively large. Two of these might be due to

¹⁵ H. K. Vonach, A. Katsanos, and J. R. Huizenga, Phys. Rev. Letters **13**, 88 (1964).

¹⁶ B. W. Allardyce *et al.*, Phys. Letters **18**, 140 (1965).

¹⁷ A. van der Woude, Nucl. Phys. **80**, 14 (1966).

¹⁸ D. W. Lang, Nucl. Phys. **72**, 461 (1965).

nonstationary cross sections (α_6 at 0° and $\alpha_5 + \alpha_6$ at 20°). The other two $\alpha_2 + \alpha_3$ and α_4 at 20°, show the influence of nonstatistical anomalies in the excitation function; these will be discussed later.

The peak-counting method⁸ of determining Γ is based on the expression

$$\Gamma_M = I b_N / 2M, \quad (6)$$

where I is the energy interval and M is the number of maxima. The values of M are given in Table II for all the excitation functions. The tabulated errors on M are subjective estimates of the uncertainties arising from experimental problems such as counting statistics. The values of b_N are given in Appendix C; they include corrections^{17,19} for energy resolution and spacing of experimental points. Finite-sample effects do not influence the b_N .¹⁷

The results of Table II reveal no consistent trend of Γ with alpha-particle group. As a working hypothesis we assume that Γ is the same for all groups. We test this hypothesis by comparing the rms deviations of the experimental values from their average with the expected standard deviations given by (B19) for Γ_A and Ref. 17 for Γ_M . This comparison is given in Table III. The standard deviation of Γ_A predicted by (B19) varies with N ; an average was used for the entries in Table III. For Γ_M , the relative standard deviation was shown in Ref. 17 to be the same for $N=1, 2,$ and 3 ; accordingly we will use the $N=1$ results of Ref. 17 for all N .

Table III shows that the measured and expected standard deviations are in agreement, so there is no evidence for a variation of Γ with alpha-particle group. Recent results of the Milan group²⁰ on $^{26}\text{Mg}(d,p)$ for deuterons from 1.5 to 3.0 MeV do show a small variation in Γ for different proton groups. The effect may be due to the large differences in channel spin and/or energy in going from one group to the next. For $^{12}\text{C}(^{16}\text{O}, \alpha)$ differences in spin and channel energy for the various exit channels are small in comparison with the amounts

¹⁹ P. G. Bizzeti and P. R. Maurenzig, Nuovo Cimento **47B**, 29 (1967).

²⁰ V. Bobyr *et al.*, Energia Nucl. (Milan) **13**, 420 (1966).

TABLE IV. Values of Γ in keV averaged over alpha-particle groups at each angle, for three intervals of bombarding energy. The standard deviation is given for each. Four anomalously large values of Γ_A were omitted. In the averages over angles each alpha group was given equal weight.

Angle (lab)	21.0-27.5 MeV		27.6-32.9 MeV		33.0-37.9 MeV	
	Γ_M	Γ_A	Γ_M	Γ_A	Γ_M	Γ_A
0°	109±12	122±16	118±26	113±19	114±14	138±17
20°	113±10	131±24	108±14	145±48	99±8	141±52
59°	107±8	126±36	113±20	96±24	91±11	111±19
149°	100±15	114±26	118±26	123±19
178°	101±10	149±36	157±26	141±23
Average over angles	107±12	128±31	113±21	118±37	109±25	130±33
Mean ^{28}Si excitation energy	27.1 MeV		29.7 MeV		32.0 MeV	
Dominant J value ^a	8 or 9		10		11	

^a See Ref. 22.

available in the final system. The differences in transmission coefficients and phase space factors are correspondingly smaller, and it is therefore not surprising that Γ shows no variation.

It may be noted from Table III that for a given sample size, $\text{RSD}(\Gamma_M) < \text{RSD}(\Gamma_A)$; this effect was noted earlier for synthetic excitation functions.¹⁷ The peak count is insensitive to effects of nonstationary cross sections and finite-sample effects. Furthermore, analysis of synthetic excitation functions shows that Γ_A is correlated with $R(0)$, tending to be large when $R(0)$ is large^{17,21}; Γ_M is uncorrelated with $R(0)$.²¹ Thus, not only is the peak-counting method a simpler and quicker

method of obtaining Γ , but it is also more reliable. Of course, if counting statistics are poor spurious maxima may appear, especially if the fluctuations are highly damped. This problem is treated in Ref. 19. It did not appear to be serious for the present data.

The variation of Γ with angle and energy is of considerable interest. To highlight these features, Γ_A and Γ_M were obtained at all five angles for three energy intervals determined by the segments of the 149° and 178° (lab) excitation functions. The numbers were then averaged over the alpha-particle groups in each interval, and the results are given in Table IV and Fig. 8. These are based on 55 values of Γ_M and 51 for Γ_A —four excessively large values of Γ_A were not used. Figure 8 also shows averages of Γ_M over groups and angles, and the expected standard deviation of Γ_M as given by van der Woude.¹⁷

The variation of Γ with angle is very small. The angle independence is explained in the following paper⁴; in brief, the spin population of the compound states tends to be so strongly peaked near on J value that contributions from the dominant spin overwhelm those from other states. Thus, the tabulated Γ values are substantially equal to Γ_J for the appropriate J value. This feature is unusual—ordinarily, measured Γ values are weighted averages over the individual Γ_J , and unfolding the J dependence is difficult. The dominant J values for the three energy ranges, calculated by the statistical model,²² are given in Table IV.

The variation of Γ with excitation energy shown by the averages over angles in Table IV is also very slight. A more exacting test for such a variation may be obtained from the results in Table V, based on halving the longest excitation functions, those at 0° and 20°. The increase of Γ_M from the lower half (mean excitation energy 28.1 MeV) to the upper half (33.0 MeV) averages about $(6 \pm 12)\%$; the variation of Γ_A is similar but with larger uncertainty.

We conclude that for our data Γ does not vary sig-

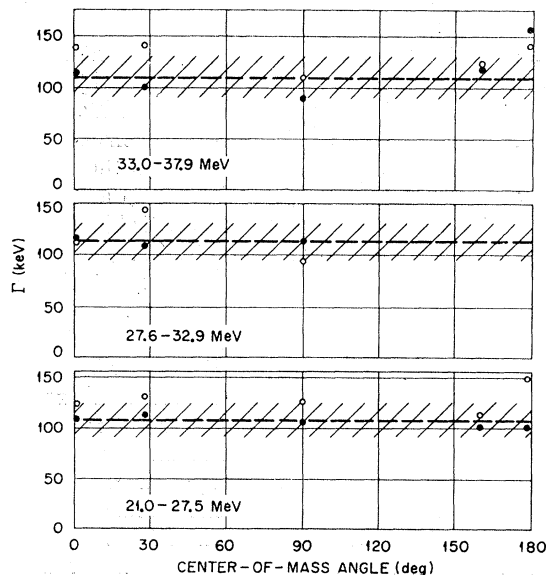


FIG. 8. Coherence widths averaged over alpha-particle groups for three energy regions. The dots are for Γ_M and the open circles for Γ_A . The dashed lines give the averages of Γ_M for all groups and angles. The hatched areas indicate the range expected for plus or minus one standard deviation of Γ_M as given in Ref. 17.

²¹ P. J. Dallimore and I. Hall, Nucl. Phys. 88, 193 (1966).

²² E. Vogt and D. McPherson (private communication).

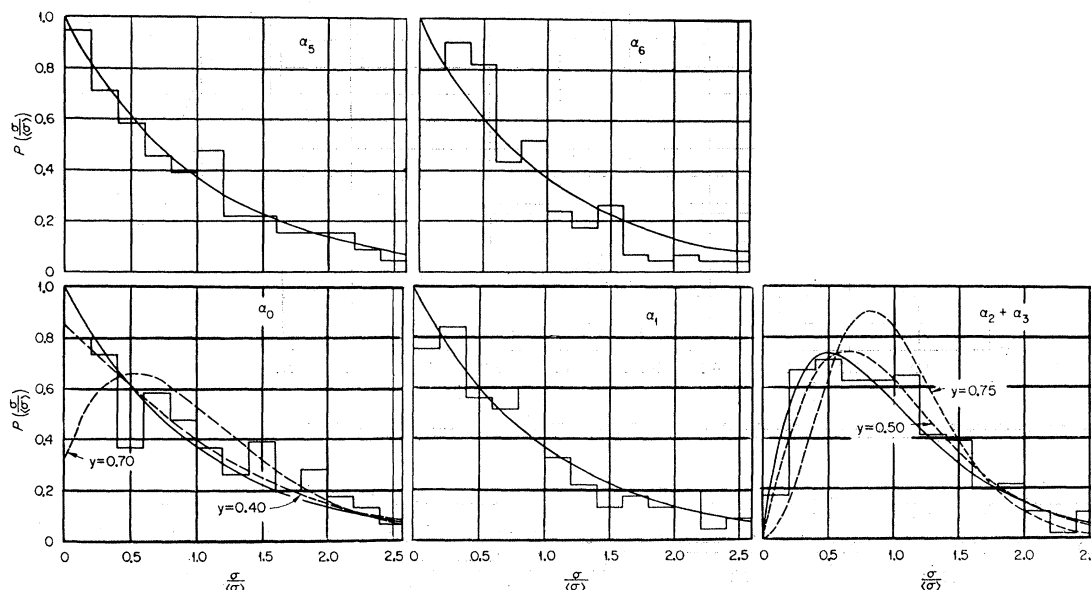


FIG. 9. Probability distributions for the data at 0° . The full curves are theoretical predictions for the appropriate N values with $y=0$. The dashed curves are for other values of y .

nificantly with excitation energy. A similar trend was observed in the reaction $^{27}\text{Al}(p, \alpha)^{24}\text{Mg}$ from 22.1 to 30.6-MeV excitation energy²³: the value of Γ increases only slightly, from about 60 keV to about 80 keV. Recent work on $^{24}\text{Mg}(\alpha, \alpha')$ from 27.8- to 32.5-MeV excitation energy shows also a small ($\sim 30\%$) increase in Γ with energy.²³ Likewise, in the reaction $^{28}\text{Si}(n, p)$ for neutron energies from 5.9 to 9.1 MeV (14 to 17 MeV in the compound system), the average number of maxima in the lower half of the energy range is practically equal to the number in the upper half,²⁴ showing that Γ does not change significantly.

On the other hand, the value of Γ measured in the reaction $^{27}\text{Al}(\alpha, p)$ doubles in going from 15- to 17-MeV excitation, and theoretical calculations follow this trend very well.²⁵ The reaction $^{27}\text{Al}(d, \alpha)$ behaves in a similar fashion: For 2-MeV deuterons (≈ 20 -MeV excitation) Γ is about 40 keV,²⁶ while for 5-MeV deuterons (≈ 23 MeV excitation) it is 1.5–2 times larger.²⁷ Again, this trend is predicted by statistical-model calculations.²⁸ Perhaps the largest change of Γ with energy thus far reported is that for $^{31}\text{P}(p, \alpha)$: Γ increases from 11 ± 1

to 95 ± 15 keV from about 14- to 29-MeV excitation.²⁹ The last-mentioned work also includes a measurement of Γ for the ^{32}S compound system at 29 MeV with the reaction $^{16}\text{O}(^{16}\text{O}, \alpha)$, namely 73 ± 7 keV. These results for ^{32}S contrast with the results for ^{28}Si in which Γ from the oxygen-induced reaction is larger than from the (p, α) reaction. No explanation has thus far been discovered for these remarkable dissimilarities in the behavior of Γ .

The average of all the Γ_M values for the three intervals of Table IV is 109.4 ± 20.1 keV, while for the 51 acceptable Γ_A values the average is 126.1 ± 33.9 keV. These error estimates are merely the standard deviations of the numbers being averaged. The weighted mean of these numbers is 117.8 ± 17.3 keV.

TABLE V. Values of Γ in keV averaged over alpha groups for the 0° and 20° excitation functions divided into halves. Certain data were omitted from the Γ_A averages, as indicated. The $\alpha_5 + \alpha_6$ data at 20° begin at 22.6 MeV.

Angle (lab)	Bombarding energy span			
	20.6–32.2 MeV		32.2–43.7 MeV	
	Γ_M	Γ_A	Γ_M	Γ_A
0°	104 ± 7	137 ± 37	121 ± 6	149 ± 9
20°	110 ± 9	129 ± 33^a	106 ± 6	139 ± 40^b
Averages over angles	107 ± 8	134 ± 36	113 ± 10	145 ± 28

^a Omitting $\alpha_2 + \alpha_3$ and α_4 .

^b Omitting $\alpha_5 + \alpha_6$.

²³ L. W. Put, J. D. A. Roeders, and A. van der Woude, in *Proceedings of the International Conference on Nuclear Physics, Gallinburg, Tennessee, 1966*, edited by R. L. Becker, C. D. Goodman, P. L. Stelson, and A. Zucker (Academic Press Inc., New York, 1967); (private communication).

²⁴ G. Andersson-Lindström and E. Rössle, *Phys. Letters* 5, 71 (1963).

²⁵ G. Dearnaley *et al.*, *Phys. Rev.* 139, B1170 (1965).

²⁶ E. Gadioli, G. M. Marazzan, and G. Pappalardo, *Phys. Letters* 11, 130 (1964).

²⁷ Y. Cassagnou *et al.*, *Phys. Letters* 8, 276 (1964).

²⁸ Y. Cassagnou *et al.*, *Phys. Letters* 6, 209 (1963).

²⁹ R. B. Leachman, P. Fessenden, and W. R. Gibbs (to be published).

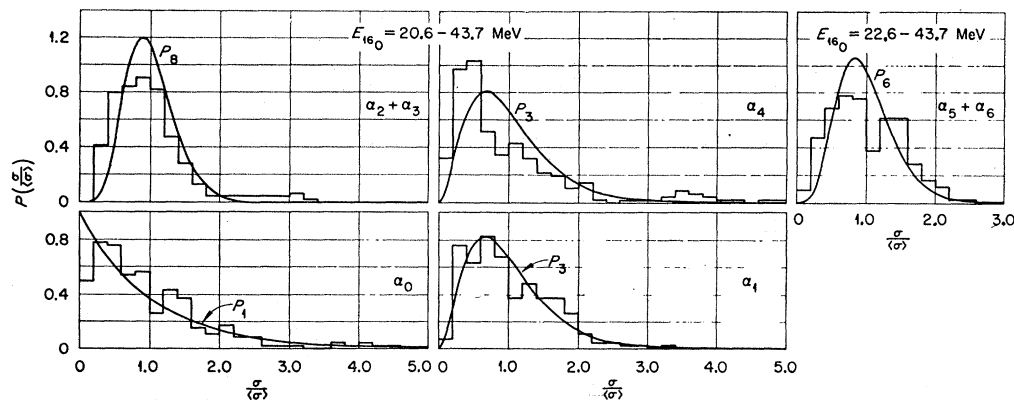


FIG. 10. Probability distributions for the data at 20° (lab). The curves are $y=0$ predictions for the indicated values of N .

C. Determination of y from Distribution Functions

For the simplified nuclear model under consideration, Ericson³⁰ and Stephen³¹ have shown that the distribution of a fluctuating cross section about its mean value $\langle\sigma\rangle$ may be characterized very simply by N and y . For $y=0$ one obtains a χ^2 distribution of $2N$ degrees of freedom for the variable $\sigma/\langle\sigma\rangle$. The χ^2 distribution is simply an exponential for $N=1$. When $N>1$, the distribution

is peaked at $\sigma/\langle\sigma\rangle=1-1/N$. For $y\neq 0$, the distributions are more sharply concentrated near $\sigma/\langle\sigma\rangle=1$, the peaking becoming more pronounced as y increases.

In Figs. 9-13, the probability distributions are presented for all the data at the various angles. For the 149° and 178° data, the upper and lower portions of the excitation functions were combined. The theoretical distributions for $y=0$ are shown by the full curves;

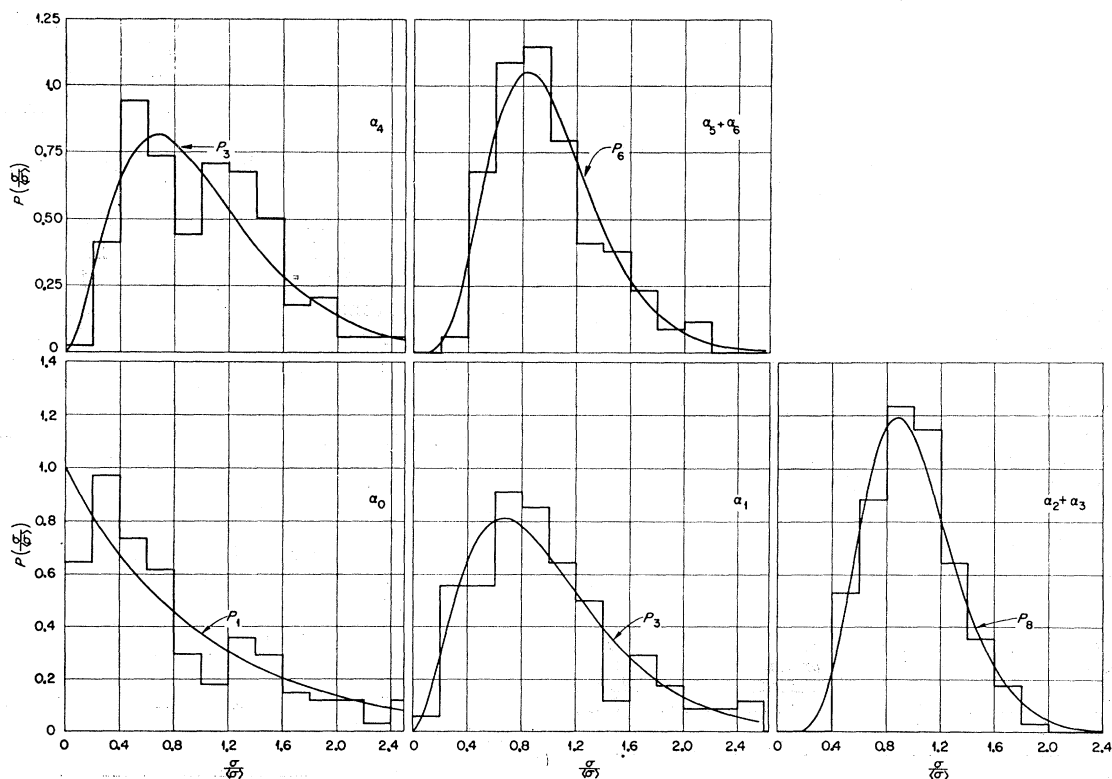


FIG. 11. Probability distributions for the data at 69° (lab). The curves are $y=0$ predictions for the indicated values of N .

³⁰ T. Ericson, Phys. Letters 4, 258 (1963).

³¹ R. O. Stephen, thesis, Oxford University, 1963 (unpublished).

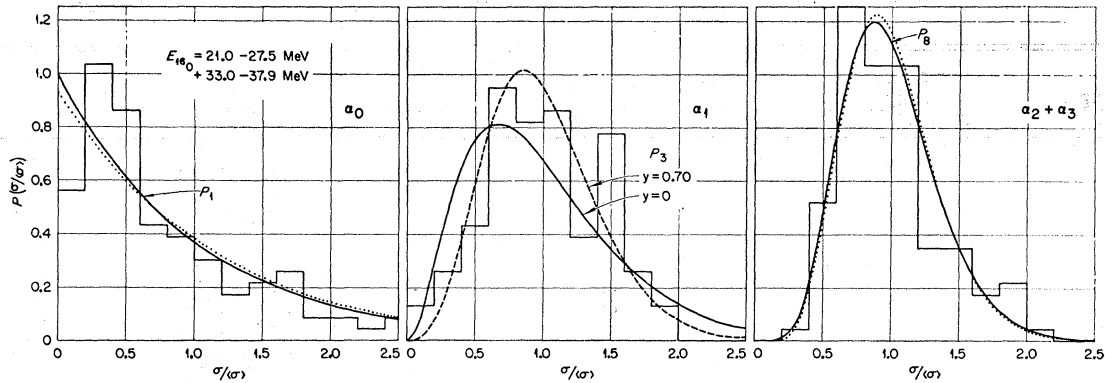


FIG. 12. Probability distributions for the data at 149° (lab). The 21.0–27.5 and 33.0–37.9 MeV segments of the excitation functions were combined. The full curves are $y=0$ predictions for the indicated values of N , while the dashed curve for α_1 shows the $y=0.70$ prediction for $N=3$. The dotted curves for α_0 and $\alpha_2+\alpha_3$ show the $y=0$ finite-sample distribution predicted for sample size $n=16$.

most of the experimental histograms are consistent with these $y=0$ distributions. The most pronounced exceptions to the general $y \approx 0$ conclusion are the α_1 data at 149° and 178°, and $\alpha_2+\alpha_3$ at 178°. The α_0 distribution at 178° is fit equally poorly by $y=0$ and $y=0.7$; this is probably a consequence of the large peak in the excitation function (Fig. 6) near 25-MeV bombarding energy. The $\alpha_2+\alpha_3$ and α_4 distributions at 20° are similar to α_0 at 178°—the fits are poor for all choices of y , and there are too many large cross sections. Again, this can be traced to the large peaks evident in the excitation functions (Fig. 3); these peaks will be discussed later.

The effect of a finite sample on the theoretical distribution function has been calculated by Gibbs³² for $y=0$. The effect is quite small for the sample sizes of interest here. The dotted curves given in Fig. 12 for α_0 and $\alpha_2+\alpha_3$ are the finite-sample distribution functions for $N=1$ and $N=8$. The sample size is $n \approx 16$ for the energy intervals combined in Fig. 12. The largest effect for the

present data occurs with the 21.0–27.5-MeV interval for $\alpha_2+\alpha_3$ at 178°, for which $n \approx 9$. The dotted curve in the right-hand section of Fig. 13 shows the corrected distribution. It is clear that for the present data the finite-sample effect is insignificant. It may be useful to state an empirical observation: The $y=0$ distribution for sample size $n \gtrsim 4$ is very similar to the distribution for infinite samples having $y=n^{-1/2}$.

D. Determination of y from $R(0)$

For $\epsilon=0$, Eq. (4) becomes

$$R(0) = (\langle \sigma^2 \rangle - \langle \sigma \rangle^2) / \langle \sigma \rangle^2. \quad (7)$$

The quantity $R(0)$ is thus a measure of the strength of the fluctuations. For infinite samples its expectation value is²

$$\bar{R}(0) = (1 - y^2) / N. \quad (8)$$

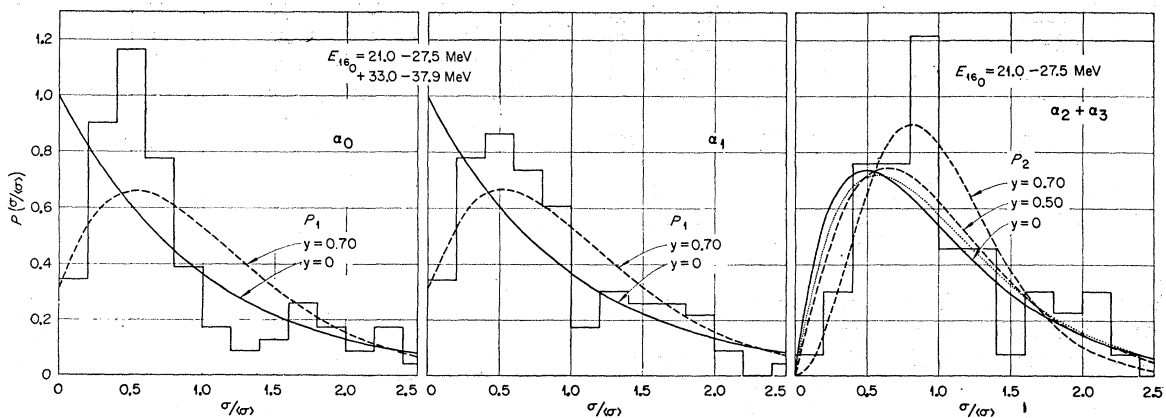


FIG. 13. Probability distributions for the data at 178° (lab). The 21.0–27.5 and 33.0–37.9 MeV segments of the excitation functions were combined. The curves show theoretical predictions for various choices of y for the indicated values of N . The dotted curve for $\alpha_2+\alpha_3$ shows the $y=0$ finite-sample distribution predicted for sample size $n=9$.

³² W. R. Gibbs, Los Alamos Scientific Laboratory Rept. No. LA-3266 (unpublished).

TABLE VI. Experimental values of $R(0)$, compared with the finite-sample expectation values and standard deviations. The quantity Q is defined by (9).

Angle (lab)	Bombarding energy span (MeV)	n	Group	$R(0)$	$\bar{R}(0)$	Q
0°	20.6-43.7	28.4	α_0	0.654	0.932 ± 0.247	-1.12
	20.6-43.7	28.4	α_1	0.843	0.932 ± 0.247	-0.36
	20.6-43.7	28.4	$\alpha_2 + \alpha_3$	0.397	0.474 ± 0.109	-0.71
	20.6-43.7	28.4	α_5	0.927	0.932 ± 0.247	-0.02
	20.6-43.7	28.4	α_6	1.060	0.932 ± 0.247	0.52
20°	20.6-43.7	28.4	α_0	0.710	0.932 ± 0.247	-0.90
	20.6-43.7	28.4	α_1	0.352	0.318 ± 0.069	0.49
	20.6-43.7	28.4	$\alpha_2 + \alpha_3$	0.317	0.120 ± 0.024	8.24
	20.6-43.7	28.4	α_4	0.854	0.318 ± 0.069	7.78
	22.6-43.7	26.0	$\alpha_5 + \alpha_6$	0.253	0.159 ± 0.034	2.78
69°	21.0-37.9	20.9	α_0	1.062	0.908 ± 0.281	0.54
	21.0-37.9	20.9	α_1	0.311	0.312 ± 0.079	-0.02
	21.0-37.9	20.9	$\alpha_2 + \alpha_3$	0.092	0.118 ± 0.027	-0.96
	21.0-37.9	20.9	α_4	0.262	0.312 ± 0.079	-0.64
	21.0-37.9	20.9	$\alpha_5 + \alpha_6$	0.152	0.157 ± 0.037	-0.15
149°	21.0-27.5	8.7	α_0	1.214	0.794 ± 0.381	1.10
	21.0-27.5	8.7	α_1	0.142	0.284 ± 0.111	-1.28
	21.0-27.5	8.7	$\alpha_2 + \alpha_3$	0.093	0.109 ± 0.039	-0.41
	33.0-37.9	6.8	α_0	0.574	0.744 ± 0.403	-0.42
	33.0-37.9	6.8	α_1	0.198	0.271 ± 0.120	0.61
178°	33.0-37.9	6.8	$\alpha_2 + \alpha_3$	0.089	0.105 ± 0.043	-0.36
	21.0-27.5	8.7	α_0	1.592	0.794 ± 0.381	2.10
	21.0-27.5	8.7	α_1	0.378	0.794 ± 0.381	-1.09
	21.0-27.5	8.7	$\alpha_2 + \alpha_3$	0.267	0.419 ± 0.174	-0.87
	33.0-37.9	6.8	α_0	0.516	0.744 ± 0.403	-0.57
	33.0-37.9	6.8	α_1	0.506	0.744 ± 0.403	-0.47

Recently it has been pointed out^{32,33} that an additional term should appear in the above expression, but this term vanishes if the fluctuating parts of the cross sections in the N channels contribute equally, as has already been assumed in this paper.

For finite samples, $\bar{R}(0)$ is biased toward values smaller than those given by (8). Appendix B presents various estimates of $\bar{R}(0)$ in comparison with results from synthetic excitation functions; we use the estimate (B7). In examining experimental results it is also necessary to have estimates of the expected spread of values about $\bar{R}(0)$ due to the sample size. We take these from (B10). It is convenient to introduce the variable Q expressing the deviation of the experimental value of $R(0)$ from the expectation value in terms of the expected standard deviation

$$Q = [R(0) - \bar{R}(0)] / \{\text{var}[R(0)]\}^{1/2}. \quad (9)$$

This variable depends on y ; for the choice of y which correctly describes the real situation, the distribution of Q values should have mean value zero and unit standard deviation.

Table VI presents $R(0)$ and related quantities for all the data. Most of the experimental values are within one or two standard deviations of the expectation value. This indicates that $y=0$ describes most of the data adequately. The exceptions are discussed in the next section.

The energy spans in Table VI are of grossly unequal length. To obtain approximately equal samples, the

³³ W. von Witsch *et al.*, Nucl. Phys. 80, 394 (1966).

data at 0°, 20°, and 69° were segmented to correspond to the energy spans of the back-angle data. The mean value and standard deviation of the resulting 55 values of Q are 0.01 ± 1.05 , in agreement with expectation for $y=0$. If the 20° data showing the anomalies discussed below are excluded, the result is -0.09 ± 0.91 , still in good agreement with the $y=0$ expectation.

E. Anomalies at 31.8 MeV

Two remarkable exceptions to the general $y=0$ trend stand out in Table VI: $R(0)$ for $\alpha_2 + \alpha_3$ and α_4 at 20° ($\sim 28^\circ$ c.m.) differs from the expectation value by 8.2 and 7.8 standard deviations, respectively. Chance occurrence of such large deviations is extremely improbable. Furthermore, as was pointed out earlier, the excitation functions for these two groups (Fig. 3) show extremely large peaks near 31.8-MeV bombarding energy, about 3.4 and 4.9 times the average cross section for $\alpha_2 + \alpha_3$ and α_4 , respectively. According to the Ericson-Brink-Stephen model, the predicted $y=0$ distributions assign probabilities of 1.4×10^{-4} and 1.3×10^{-4} for chance occurrence of such large cross sections. The width of these peaks is large, 5 or 6 Γ , and therefore each should be regarded as two substantially independent pieces of data. The probabilities are then of the order of 10^{-8} . If $y \neq 0$, they are even smaller. Furthermore, the peaks occur at the same energy for both groups. We conclude that it is extremely unlikely that the peaks represent merely random fluctuations within our simplified model.

The 31.8-MeV behavior of the excitation functions at other angles does not seem unusual. At 0° and 69° , peaks appear in the $\alpha_2+\alpha_3$ and a few other excitation functions at 31.8 MeV, but $\sigma/\langle\sigma\rangle$ is within normal statistical limits. The 149° and 178° excitation functions for $\alpha_2+\alpha_3$ and α_4 do not cover energies in this neighborhood. The angular distributions of Ref. 4 do span these energies, but a careful examination of these data did not lead to any simple conclusions about the angular distribution of the 31.8-MeV anomalies.

To study the anomalous peaks further, the measured cross sections at 0° , 20° , and 69° were summed over all the alpha-particle groups to damp the fluctuations. Figure 14 shows the results. The average trend of the cross sections is a slow increase and then a slow decrease with energy. These are probably due to the increase of cross section in the entrance channel as the Coulomb barrier (~ 22 MeV lab) is crossed, and then the effect of competition from the opening of new exit channels as the energy continues to increase.

The anomaly at 31.8-MeV bombarding energy is clearly evident at 20° , but missing at 69° . The sum of the 0° data shows its strongest peak at 31.8 MeV even though the peaks in the individual excitation function are within normal statistical limits. This indicates that there is a coherent effect in different exit channels at this energy. According to our simplified model, the probability of random occurrence of such a large peak is only 1.2% if the sum is assumed to be made up of six equally intense, statistically incoherent $\gamma=0$ cross sections. Furthermore, the probability that a peak of width $\sim\Gamma$ might appear by chance at the same energy as the one at 20° is $1/84$, if we assume equal probability for any portion of the full interval of length 84Γ . Thus, the chance that the 0° peak at 31.8 MeV is purely a random fluctuation is only 0.00014.

Additional peaks appear in the 0° sum, notably at 36.4- and 37.6-MeV bombarding energy. Their probabilities for chance occurrence are 10.1% and 4.6%, respectively, so it seems likely that these peaks are consistent with our statistical model.

The 31.8-MeV peaks may not be anomalous within the framework of the more accurate *R*-matrix models discussed by Moldauer.¹⁰ Qualitatively, the behavior of these peaks is consistent with predictions of Ref. 10: The peaks appear at the same energy in more than one exit channel, and they tend to be broader than the average Γ . Near 31.8 MeV the damping of the fluctuations in the angle integrated cross section for $\alpha_2+\alpha_3$ is weaker than for the other groups, and in fact suggests that only one partial wave is important.⁴ At present, however, we do not know how to make a quantitative test to judge whether the 31.8 MeV peaks fall within normal limits for some *R*-matrix models.

F. Average Cross Sections

The average cross section $\langle\sigma\rangle$ for a finite sample is an unbiased estimator of the infinite-sample average cross

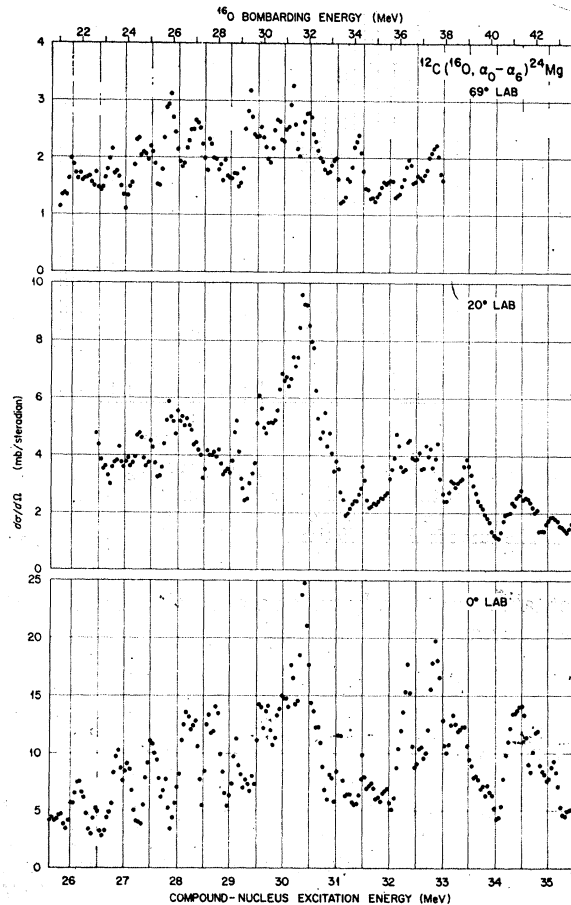


FIG. 14. Sums of excitation functions at three angles for all groups up to and including α_6 .

section, $\bar{\sigma}$.⁵ Therefore, the experimental values of $\langle\sigma\rangle$ given in Table II may be compared directly with compound-nucleus calculations of the average cross section. For such a comparison it is necessary to know the variance expected for $\langle\sigma\rangle$. In this work we use expression (B5). The experimental $N=1$ average cross sections may be expected to deviate from the calculated averages by as much as 20% (40%) for the longest (shortest) intervals of interest here.

Vogt and McPherson have made statistical-model calculations of average cross sections for this reaction.²² Reasonable starting estimates of the level-density parameters were adjusted to give good fits to our observed α_0 and α_1 cross sections at 0° . These parameters were then used to calculate all other cross sections. Most of the results were within a factor of 2 or 3 of the measured values. These discrepancies are larger than the statistical uncertainties predicted by (B5), but in view of the extreme sensitivity of such calculations to the choice of level-density parameters it seems likely that further small adjustments could easily improve the fits. Such attempts at refinement were felt to be un-

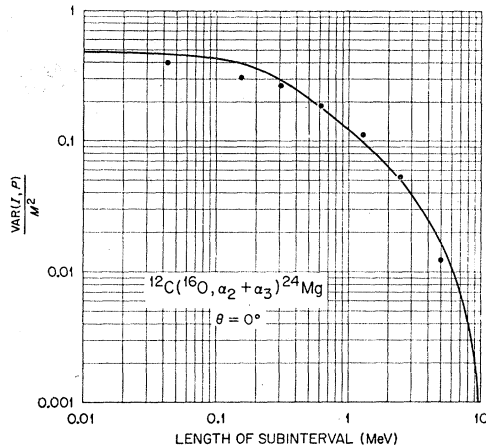


FIG. 15. Variance of zero-degree $\alpha_2 + \alpha_3$ average cross sections for various partitions P of the excitation function. The quantity M is the experimental average cross section for the full range of data. The curve is the prediction for $\Gamma = 120$ keV, $N = 2$, and $\gamma = 0$.

profitable, particularly since data on other exit channels are not available.

G. Subinterval Averages

The data offer a possibility of a test of (B5).³⁴ The full energy span I was partitioned into P subintervals, the value of $\langle \sigma \rangle_{I/P}$ for each subinterval calculated, and the variance of these subinterval averages determined. The process was repeated for other choices of P . In Figs. 15 and 16 the results for the 0° data are compared with theoretical predictions for $\gamma = 0$ and $\Gamma = 120$ keV. The curves are based on a modification³⁵ of (B5). The modification is necessary because the experimental variances are calculated with respect to $\langle \sigma \rangle_I$ instead of $\bar{\sigma}$, which is unknown. The agreement with the assumed parameters is satisfactory—the scatter of the experimental values is within expected limits.³⁶

Böhning³⁴ developed an elaboration of this method of finding Γ and γ [or more precisely, $(1 - \gamma^2)/N$] by means of a least-squares-fitting procedure. A comparison of the parameters obtained in this way with those determined by other methods would provide a test of the model adopted to represent the compound system. Böhning found that for the present data the best-fit values of Γ and γ do in fact agree with the other determinations, but the statistical reliability of simultaneous determination of the two parameters is unfortunately inadequate to provide a good check of the model.³⁶ As a further application, consideration was given to estimation of I for data taken with poor energy resolution since the conventional methods are then unreliable.^{34,35} Again, it was found that if γ and N are not known *a priori*, the method is not reliable.³⁶ A somewhat similar

³⁴ M. L. Halbert and M. Böhning, Bull. Am. Phys. Soc. **10**, 120 (1965).

³⁵ Oak Ridge National Laboratory Rept. No. ORNL-3800, pp. 33–35 (unpublished).

³⁶ M. Böhning (private communication).

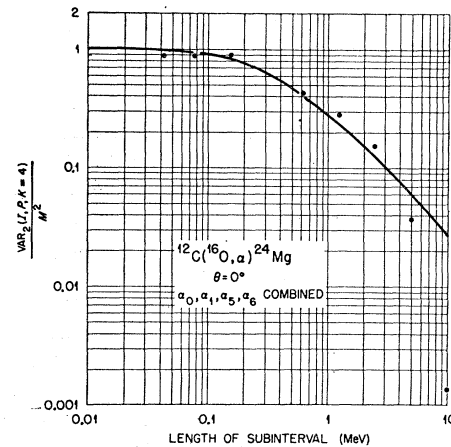


FIG. 16. Variance of the four $N = 1$ zero-degree cross sections for various partitions P of the excitation functions. The quantity M is the mean value of the energy-averaged cross sections for the four groups. The curve is the prediction for $\Gamma = 120$ keV, $N = 1$, and $\gamma = 0$.

concept has been used³⁷ to extract 0.1-keV widths from data taken with 6-keV resolution by means of a formula equivalent to (B5). This procedure is likewise completely dependent on prior knowledge of γ and N .

V. SUMMARY AND CONCLUSIONS

Excitation functions for alpha-particle groups corresponding to low-lying states of ^{24}Mg were measured for the reaction $^{12}\text{C}(^{16}\text{O}, \alpha)^{24}\text{Mg}$. The compound-nucleus excitation energies cover the region 25–35 MeV. Pronounced fluctuations were observed which were analyzed in terms of the statistical model used by Ericson, and by Brink and Stephen.

Within uncertainties governed mainly by the sample size, the coherence width Γ is the same for all exit channels. There is no significant evidence for a variation of Γ with angle or compound-nucleus excitation. The latter conclusion is in agreement with some results on similar compound systems, but in strong disagreement with others, for unknown reasons. Two methods were used to obtain Γ : measuring the widths of autocorrelation functions and counting of maxima in the excitation functions. They gave practically the same result, provided that appropriate finite-sample corrections were included and a recently modified version of the relation between Γ and the number of maxima was used. The spread of the experimental Γ values about the mean is substantially smaller for the peak-counting results, in agreement with recent analyses of synthetic excitation functions. The over-all average result is $I = 117.8 \pm 17.3$ keV. This width is characteristic mainly of compound levels with spin ~ 10 .

The nonfluctuating (direct-interaction) component γ of the average cross section was found to be generally

³⁷ P. Fessenden, W. R. Gibbs, and R. B. Leachman, Phys. Rev. Letters **15**, 796 (1965).

consistent with zero. Two pieces of evidence lead to this conclusion: the distribution functions agree with the $y=0$ prediction, and the variances of the cross section [i.e., the values of $R(0)$] are, in practically all cases, within one or two standard deviations of the expectation values for $y=0$.

The energy-averaged cross sections are in satisfactory agreement with statistical-model calculations. The variances shown by the data are consistent with that expected for cross-section averages over finite energy intervals.

Unusually large peaks occur at 31.8-MeV bombarding energy in two excitation functions at 20° , and in the sums of the measured cross sections at 0° and 20° . These peaks constitute pronounced exceptions to the general success of the simplified statistical model. Since a fluctuation theory can merely demonstrate that certain behavior falls outside its scope and cannot explain the underlying mechanism, the physical significance of the 31.8-MeV anomalies remains unclear. It is possible that with a more accurate statistical model they would no longer appear anomalous. Striking as this behavior may be, however, it should not obscure the fact that the simple Ericson-Brink-Stephen model is well suited for the great bulk of the data reported here.

ACKNOWLEDGMENTS

The 0° and 20° data were obtained in collaboration with C. D. Moak and A. Zucker. We wish to thank them for the long hours they put in on this project, and for their continuing interest in its outcome. M. Böhning was especially helpful during many phases of the analysis and we thank him for his patience in providing detailed explanations of theoretical points and much unpublished material. We acknowledge with gratitude our debt to the operating crew of the tandem accelerator under G. F. Wells. Many other persons assisted in one way or another with the accumulation and processing of the data, including L. C. Becker, C. R. Bingham, I. M. Brann, D. O. Galde, G. A. Palmer, W. J. Roberts, and T. P. Whaley. Correspondence and discussion with W. R. Gibbs, I. Hall, C. Mayer-Böricke, J. A. Kuehner, and the late E. Almqvist were helpful. We should also like to thank E. Vogt and D. McPherson for the statistical model calculations. Finally, we extend our thanks to E. C. Halbert, W. R. Gibbs, and R. B. Leachman for many suggestions to improve the manuscript. One of us (A. v.d. W.) would like to acknowledge a NATO fellowship administered by the "Nederlandse Organisatie voor Zuiver Wetenschappelijk Onderzoek" during part of his stay at Oak Ridge National Laboratory.

APPENDIX A: ESTIMATE OF Γ/D

One of the basic assumptions of the Ericson-Brink-Stephen fluctuation theory is that the compound levels are strongly overlapping. The cross-section fluctuations are then due solely to interference among nearby com-

pound-nuclear levels. If the overlap is not strong, the strength of the fluctuations is increased because of random variations of level density with energy. This situation has been studied by Moldauer³⁸ for $N=1$ and arbitrary y , and by Dallimore and Hall²¹ for $N=1$ to 4 with $y=0$. In the latter investigation, made by means of synthetic excitation functions, the effect was found to be negligible even for Γ/D as small as 2. The authors point out, however, that due to restrictions they placed on their reaction amplitudes and on their distribution of compound-level spacings, the effect should be zero or close to it. Moldauer's assumptions, particularly for the level-spacing distribution, are more general; therefore we will use his results for judging compliance with the strong-overlap condition.

Moldauer's $N=1$ result for $\text{var}\sigma$ can be written

$$\text{var}\sigma = \bar{\sigma}^2 \{ (1-y^2) + [f(\Gamma/D) - 1](1-y)^2 \}. \quad (\text{A1})$$

The function f is about 3 for $\Gamma/D=1$, about 1.1 for $\Gamma/D=10$ and approaches 1.0 for $\Gamma \gg D$. In the latter limit, the second term in curly brackets vanishes, leaving the usual Ericson expression for $N=1$. Finite-sample effects are excluded for these calculations, so that the autocorrelation is given by

$$R(0) = \text{var}\sigma / \bar{\sigma}^2. \quad (\text{A2})$$

The effect of weak overlap is largest for $y=0$, in which case

$$R(0) = f(\Gamma/D). \quad (\text{A3})$$

Thus if $\Gamma \approx D$, the autocorrelation is about three times larger than for $\Gamma \gg D$.

Estimation of Γ/D from the statistical theory is very difficult. It was decided instead to make only a consistency check of Γ/D at 25 MeV, the lowest excitation energy for the fluctuation analysis. The average spacing was estimated as described below and compared with the measured Γ to check whether Γ/D was sufficiently large to justify the fluctuation analysis.

The estimate of D was made by fitting the expression³⁹

$$\rho(E) = CE^{-5/4} \exp[2(aE)^{1/2}] \quad (\text{A4})$$

to the density of known ^{28}Si levels up to 14 MeV. A good fit was obtained with $a=3.2 \pm 0.2 \text{ MeV}^{-1}$ and $C=0.0021 \mp 0.0008 \text{ MeV}^{-1}$, the last figure showing the range of C values required for a fit with the extreme values of a . At 25 MeV, the average spacing D is then 0.45 keV. This estimate is surprisingly insensitive to the details of the fitting procedure. For example, a fit with pre-exponential factor³⁹ of E^{-2} instead of $E^{-5/4}$ gave the same value of D within 10%.

The dominant spin value at this energy is about 8.²² The experimental width $\Gamma \approx 118 \text{ keV}$ should be typical of compound levels with $J \sim 8$. We adopt the usual Gaussian spin dependence for the level density³⁹

$$\rho(E, J) = \rho(E, 0) (2J+1) e^{-J(J+1)/2\sigma^2}. \quad (\text{A5})$$

³⁸ P. A. Moldauer, Phys. Letters 8, 70 (1964).

³⁹ T. Ericson, Advan. Phys. 9, 425 (1960), Eq. (3.15).

The spin cutoff parameter σ is given by

$$\sigma^2 = \mathcal{J}T/\hbar^2, \quad (\text{A6})$$

where \mathcal{J} is the moment of inertia (here taken as the moment for a rigid sphere with radius parameter 1.22 F) and T is defined by

$$1/T = d \log \rho(E)/dE. \quad (\text{A7})$$

For the present case these parameters are $T=3.25$ MeV and $\sigma^2=11.6$. To relate this partial density $\rho(E, J)$ to the total density $\rho(E)$ estimated previously, we note that $\rho(E, 0)$ is approximately equal to $\rho(E)/2\sigma^2$, as can be shown by equating

$$\sum_{J=0}^{\infty} \rho(E, J)$$

to $\rho(E)$.⁴⁰ Then D_J for $J=8$ is 14.3 keV, and $\Gamma/D_8 \approx 8.3$. This estimate is subject to large error, of course, because of the uncertainty of the extrapolation from the region of isolated levels. However, since it is likely that levels were missed in the 12–14 MeV experiments, it is more probable that we have an underestimate of Γ/D rather than an overestimate. It thus seems safe to apply the expressions derived for $\Gamma \gg D$, since the Moldauer correction is $\lesssim 10\%$.

With models other than the Ericson–Brink–Stephen model, the conditions on Γ/D may be more stringent. For the “ R -matrix models,” Γ/D may have to be very much larger in order to use the $\Gamma \gg D$ expressions safely.¹⁰

APPENDIX B: FINITE-SAMPLE EFFECTS

A number of authors have considered finite-sample biases and variances for the simplified model described in Sec. IV. It is the purpose of this Appendix to compare the various results and select from among them those to be used in the analysis of the $^{12}\text{C}(^{16}\text{O}, \alpha)$ data.

1. Average Cross Section

Böhning⁵ has shown that $\langle \sigma \rangle_I$, the cross section averaged over an interval I , is an unbiased estimator of the ensemble-average cross section $\bar{\sigma}$

$$\bar{\sigma} = \langle \sigma \rangle, \quad (\text{B1})$$

and for $N=1$, and $y=0$

$$\text{var} \sigma = \bar{\sigma}^2/n, \quad (\text{B2})$$

where

$$n = \frac{I/\Gamma}{2 \tan^{-1}(I/\Gamma) - (\Gamma/I) \ln[1 + (I/\Gamma)^2]}. \quad (\text{B3})$$

This expression is exact for the model introduced in Sec. IV. The quantity n may be identified as the sample size, and to a good approximation^{7,32} it may be repre-

⁴⁰ H. K. Vonach and J. R. Huizenga, Phys. Rev. 138, B1372 (1965).

sented by

$$n \cong (I/\pi\Gamma) + 1. \quad (\text{B4})$$

If fluctuation damping is present, (B2) may be replaced approximately by³⁶

$$\text{var} \sigma = \frac{1 - y^2 \bar{\sigma}^2}{N n}. \quad (\text{B5})$$

The $y=0$ version of this relation is given in Ref. 21.

2. Expectation Value of $R(0)$

The expectation value of $R(0)$ has not been calculated exactly even for the simplified model of Sec. IV. Böhning⁴¹ has given the following expression for $y=0$ which is exact to first order in Γ/I :

$$\bar{R}(0) = \frac{1}{N} \left[1 - \frac{(1+1/N)}{(I/\pi\Gamma)} \right]. \quad (\text{B6})$$

Reference 41 also contains $\bar{R}(0)$ for $N=1$, $y \neq 0$ in the same approximation. However, in many situations of practical interest, I/Γ may not be sufficiently large to negate the importance of higher-order terms. If it is assumed that the bias of $R(0)$ is uncorrelated with the average cross section, the $y=0$ calculation simplifies markedly. It can then be shown^{21,42} that even for small n

$$\bar{R}(0) = \frac{1}{N} \left[1 - \frac{(1+1/N)/n}{(1+1/Nn)} \right] = \frac{n-1}{1+nN}, \quad (\text{B7})$$

where n is given by (B3). If this is expanded in powers of Γ/I , the leading term is in agreement with (B6).

Applying Monte Carlo methods to cross-section distribution functions, Gibbs^{7,32} arrived at the following empirical expression for $n \geq 4$, $y=0$, and $N=1, 2, 3$:

$$\bar{R}(0) = \frac{1}{N} \frac{(n-1)(4n-4+N)}{4n^2}. \quad (\text{B8})$$

Since an equally good fit to the Monte Carlo results can be obtained with (B7),⁴² and since (B7) has the correct $1/N$ dependence while (B8) does not, (B8) will not be considered further.

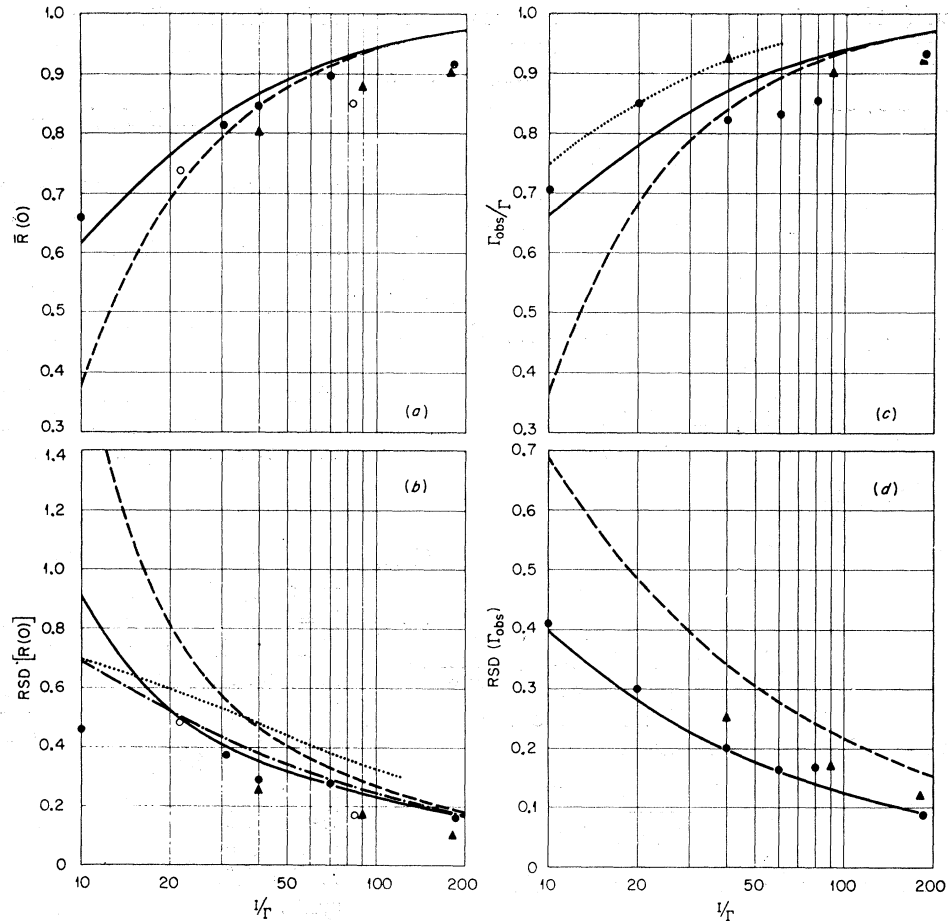
Figure 17(a) compares (B6) (dashed curve) and (B7) (full curve) for $N=1$. It is evident that (B6) approaches (B7) rather slowly. If $(I/\pi\Gamma)$ in (B6) is replaced by $(I/\pi\Gamma+1)$, the result lies about halfway between the two curves. The difference between (B6) and (B7) becomes smaller as N increases.

The full circles are from new analyses of $N=1$ synthetic excitation functions generated previously¹⁷ for compound levels distributed uniformly in energy; the triangles are for a Wigner distribution. For $I/\Gamma \geq 30$, (B6) and (B7) are equally good representations of these points. Since (B7) gives a better fit to the point at

⁴¹ M. Böhning, in Proceedings of the German Physical Society, Bad Pyrmont, 1965 (unpublished); Jahresbericht 1965, Max-Planck-Institut für Kernphysik, Heidelberg, p. 105 (unpublished).

⁴² W. R. Gibbs (private communication).

FIG. 17. Predictions and empirical results for the expectation value and relative standard deviation of $R(0)$ and the observed autocorrelation width. These are all for $N=1$ and are presented as a function of interval length divided by Γ . The full points are from the synthetic excitation functions of Ref. 17, the circles being for a uniform distribution of compound-nucleus level spacings and the triangles for a Wigner distribution. The open circles in (a) and (b) are from experimental data for $^{12}\text{C}(^{16}\text{O}, \alpha)$. The predictions are given by the various curves; each is identified in Appendix B.



$I/\Gamma=10$, it was selected for analysis of the $^{12}\text{C}(^{16}\text{O}, \alpha)$ data.

Two experimental points from the present results are also shown for comparison; they are indicated by open circles. The point at $I/\Gamma \sim 22$ is the average of 22 experimental $R(0)$ values. All the $N=1$ data for the three energy intervals determined by the segments of the back-angle excitation functions were used to calculate this average. The other experimental point is an average over the five $N=1$ excitation functions at 0° and 20° . The agreement with the other points is good.

3. Variance of $R(0)$

The $y=0$ variance of $R(0)$ has been given by Böhning⁴¹ to order Γ/I

$$\text{var}R(0) = \frac{1+1/N}{(I/\pi\Gamma)N^2}. \quad (\text{B9})$$

Dallimore and Hall²¹ assumed that the standard deviation is not correlated with the average cross section and arrived at a $y=0$ result for $\text{var}R(0)$ suitable for small as well as large samples. The leading term of their expression [the equation following their Eq. (3)] is given correctly by (B9), but evidently the higher terms are

important for intervals of practical interest—even for $I=100\Gamma$, (B9) is 32% larger. However, the higher-order terms given by Dallimore and Hall may be inaccurate because the no-correlation assumption cannot be expected to be valid to high order.

Figure 17(b) contains plots of $\text{RSD}[R(0)]$ for $N=1$. The dashed curve is the square root of (B9) divided by (B6), while the full curve is the square root of the Dallimore-Hall expression²¹ divided by (B7). The Monte Carlo results of Gibbs are indicated by the dotted curve; in this case $\text{var}R(0)$ was taken from Fig. 1 of Ref. 7 (Fig. 5 of Ref. 32), and its square root was divided by (B7). We also include (dash-dot curve) an approximate form based on a formula given by Dallimore and Hall in an earlier paper,⁴⁸ namely

$$\text{RSD}[R(0)] = [(1+1/N)/n]^{1/2}. \quad (\text{B10})$$

This appears to be a reasonably close approximation to the full curve for $I/\Gamma \gtrsim 15$ and the approximation becomes better for large N .

The $N=1$ results from the synthetic excitation functions and from the present experimental data are designated by the same symbols as for Fig. 17(a). Express-

⁴⁸ P. J. Dallimore and I. Hall, Phys. Letters 18, 138 (1965).

sion (B10) gives at least as good a representation of these points as any of the other expressions, and in view of its simplicity it was used in the analysis of the $^{12}\text{C}(^{16}\text{O},\alpha)$ data.

4. Autocorrelation Width

Let Γ be the true coherence width and Γ_{obs} be the width at half-maximum of the autocorrelation function, that is,

$$R(\Gamma_{\text{obs}}) = R(0)/2. \quad (\text{B11})$$

From the properties of $R(\epsilon)$ near Γ_{obs} , Gibbs has shown⁴² that for $y=0$

$$\frac{\Gamma_{\text{obs}}}{\Gamma} = \left[\frac{N\bar{R}(0)}{2 - N\bar{R}(0)} \right]^{1/2}. \quad (\text{B12})$$

Combining this with (B7) we obtain

$$\frac{\Gamma_{\text{obs}}}{\Gamma} = \left[\frac{N(n-1)}{N(n+1)+2} \right]^{1/2}. \quad (\text{B13})$$

To arrive at this result it was assumed that the finite-sample bias of $R(\epsilon)$ is the same for $\epsilon \approx \Gamma_{\text{obs}}$ as for $\epsilon=0$; this seems to be a reasonable approximation.^{36,42}

Böhning has taken a different approach.⁴¹ He considers the following estimator of Γ :

$$H(\epsilon) = \epsilon \left[\frac{R(\epsilon)}{R(0) - R(\epsilon)} \right]^{1/2}. \quad (\text{B14})$$

To first order in Γ/I , the expectation value is

$$\bar{H}(\epsilon) = \Gamma \left[1 - \frac{1 + (\epsilon/\Gamma)^2}{2I/\pi\Gamma} \left(1 + \frac{1}{N} \right) \right]. \quad (\text{B15})$$

For $\epsilon \approx \Gamma$, $\bar{H}(\epsilon) \approx \Gamma_{\text{obs}}$ and (B15) becomes

$$\frac{\Gamma_{\text{obs}}}{\Gamma} = 1 - \frac{1 + 1/N}{I/\pi\Gamma}. \quad (\text{B16})$$

Figure 17(c) gives a comparison of (B13) (full curve) and (B16) (dashed curve) for $N=1$. For $I \gg \Gamma$ they coincide, as they should. The dotted curve is copied from Fig. 5 of Ref. 21; this is the result of a calculation based on an assumption similar to that used to obtain (B7).

On the whole (B13) gives the best representation of the points from the synthetic excitation functions,¹⁷ so it was used in the analysis of the experimental data.

5. Variance of Autocorrelation Width

The $y=0$ variance of $H(\epsilon)$ is given to first order by the relation⁴¹

$$\text{var}H(\epsilon) = \frac{\Gamma^2}{4} \frac{1 + 2(\epsilon/\Gamma)^2}{I/\pi\Gamma} \left(1 + \frac{1}{N} \right). \quad (\text{B17})$$

We obtain $\text{var}\Gamma_{\text{obs}}$ by putting $\epsilon \approx \Gamma$. Dividing this by the square of (B16) for $\epsilon \approx \Gamma$ and taking only the highest-

order term in Γ/I , we obtain the square of the relative standard deviation, so that

$$\text{RSD}(\Gamma_{\text{obs}}) = \left[\frac{3(1+1/N)}{4I/\pi\Gamma} \right]^{1/2}. \quad (\text{B18})$$

The dashed curve in Fig. 17(d) shows this expression for $N=1$. The points are from synthetic excitation functions.¹⁷ The full line is the $N=1$ version of

$$\text{RSD}(\Gamma_{\text{obs}}) = \left[\frac{(1+1/N)}{4I/\pi\Gamma} \right]^{1/2}, \quad (\text{B19})$$

which gives a good representation of the points for small as well as large samples. The latter expression was used for analyzing the present experimental data.

APPENDIX C: CHOICE OF b_N

As originally presented,³ the constants b_N in Eq. (6) were $b_1=1.00$, $b_2=0.78$, $b_3=0.75$, $b_4=0.74, \dots$, $b_\infty=0.707$. However, the decrease of b_N with N appears to be much weaker on both empirical and theoretical grounds. The α_0 and α_1 excitation functions at 0° are of almost equal intensity and have 41 ± 2 and 42 ± 2 maxima, respectively. An $N=2$ excitation function was constructed by adding these together; the result had 38 ± 3 maxima rather than 32, the number expected if $b_2=0.78$. Similarly, if all the 0° excitation functions are added ($N=6$), the resultant has 39 ± 2 maxima, whereas for $b_6 \approx 0.73$, one would expect only 29. Results from synthetic excitation functions¹⁷ also show very slight dependence on N .

In an idealized situation (perfect energy resolution and infinitesimal spacing of data points) it has been recently shown analytically¹⁹ that b_N is equal to $(2\sqrt{3})/\pi = 1.1026$, independent of N . A similar result was obtained by D. M. Brink, as mentioned in a footnote of Refs. 21 and 43. For small N this is consistent with observations from synthetic excitation functions, but the latter show a small decrease in b_N as N increases.¹⁷

If data are obtained with finite energy spacing and resolution, some maxima may be missed. Therefore, b_N must be reduced.^{17,19} The corrections were made as follows. The spacing was about 0.37Γ , for which $b_1=0.95$ from Ref. 19. The finite energy resolution of $\sim 0.39 \Gamma$ reduces b_1 by a factor¹⁷ of about 0.96. We therefore took $b_1=0.91$ for our calculations. For $N > 1$, b_N/b_1 from Ref. 17 was used to calculate b_N . The results were

$$\begin{aligned} b_1 &= b_2 = 0.91, \\ b_3 &= 0.90, \\ b_6 &= 0.89, \\ b_8 &= 0.88. \end{aligned}$$

These values of b_N were used in the analysis of the $^{12}\text{C}(^{16}\text{O},\alpha)$ data.